HHS Public Access

Author manuscript

Mol Cell Endocrinol. Author manuscript; available in PMC 2016 February 05.

Published in final edited form as:

Mol Cell Endocrinol. 2015 February 5; 401: 130–141. doi:10.1016/j.mce.2014.10.017.

Regulation of cytokine-inducible SH2-containing protein (CIS) by ubiquitination and Elongin B/C interaction

Philip J. Jensik and **Lydia A. Arbogast**

Department of Physiology, Southern Illinois University School of Medicine, 1135 Lincoln Drive, Carbondale, IL, USA 62901-6523

Philip J. Jensik: pjensik@siu.edu; Lydia A. Arbogast: larbogast@siumed.edu

Abstract

Cytokine-inducible SH2-containing protein (CIS) inhibits prolactin receptor (PRLR) signaling and acts as part of an E3 ubiquitin ligase complex through interactions with Elongin B/C proteins. This study aimed to identify CIS lysine ubiquitination sites and determine roles of ubiquitination and Elongin B/C interactions on CIS protein stability and PRLR signaling inhibition. Site-directed mutations revealed that CIS can be ubiquitinated on all six lysine residues. Elongin B/C interaction box mutation had no influence on CIS ubiquitination. CIS stability was increased by mutation of lysine residues and further enhanced by co-mutation of Elongin B/C interaction domain. CIS inhibition of STAT5B phosphorylation and casein promoter activation was dependent on CIS interactions with Elongin B/C, but not on CIS ubiquitination. These data indicate CIS protein stability is regulated through multiple mechanisms, including ubiquitination and interaction with Elongin B/C proteins, whereas CIS functional inhibition of PRLR signaling is dependent on the Elongin B/C interaction.

Keywords

CIS; prolactin receptor; ubiquitination; signal transduction; STAT5; protein degradation

Introduction

Cytokine-inducible SH2-containing protein (CIS) is a member of the Suppressors of Cytokine Signaling (SOCS) family (Masuhara et al., 1997; Matsumoto et al., 1997; Starr et al., 1997; Yoshimura et al., 1995). A major function of this family is inhibition of cytokine receptor signaling (Piessevaux et al., 2008a, 2008b). Transcriptional activation of SOCS genes usually occurs by the same cytokine signaling pathways they inhibit (Matsumoto et al., 1997; Pezet et al., 1999; Tollet-Egnell et al., 1999). Each SOCS protein has a related

Corresponding author: Lydia A. Arbogast, Department of Physiology, Southern Illinois University School of Medicine, 1135 Lincoln Drive, Carbondale, IL, USA, 62901-6523 Tel: (618) 453-1856; Fax: (618)-453-1527; larbogast@siumed.edu.

structure consisting of a SH2 domain and a C-terminal SOCS box (Hilton et al., 1998; Starr et al., 1997). The SH2 domain is necessary for interaction with phosphorylated tyrosine residues on cytokine receptors (Yoshimura et al., 1995). CIS inhibits a number of cytokine signaling pathways including prolactin (PRL) and growth hormone receptor signaling (Dif et al., 2001; Ram and Waxman, 1999). CIS binds to a phospho-tyrosine residue near the signal transducer and activator of transcription 5 (STAT5) binding site and inhibits STAT5 interaction with the PRL receptor (PRLR) (Endo et al., 2003; Mayr et al., 1998). CIS suppresses growth hormone receptor signaling through multiple mechanisms, including receptor internalization via an ubiquitin-dependent pathway and inhibition of STAT5 phosphorylation by competition at receptor phosphorylated tyrosine residues (Landsman and Waxman, 2005; Ram and Waxman, 1999, 2000).

The SOCS box is involved in the formation of an E3 ubiquitin ligase complex with Elongin B/C, Cullin (CUL), and ring finger (RBX) proteins (Babon et al., 2008; Kamura et al., 1998, 2004; Piessevaux et al., 2008a, 2008b; Zhang et al., 1999). SOCS proteins function as part of the E3 ubiquitin ligase complex, increasing the degradation of a number of proteins. SOCS1 increases the degradation of translocation ets leukemia- Janus kinase 2 (JAK2) fusion protein and insulin receptor substrates 1/ 2 and this activity is dependent on the SOCS box (Kamizono et al., 2001; Rui et al., 2002). SOCS3 increases the degradation of insulin receptor substrates 1/2 and CIS has been shown to increase the degradation of growth hormone receptor, erythropoietin receptor, and Bcl-2-interacting mediator of cell death extra long (Ram and Waxman, 2000; Rui et al., 2002; Verdier et al., 1998; Zhang et al., 2008). Growth hormone stimulation also leads to CIS proteasomal degradation (Ram and Waxman, 2000). Interactions of CIS and the other SOCS proteins with the E3 ubiquitin ligase occur through the adjacent B/C and Cul boxes located within the SOCS box (Kamura et al., 2004; Piessevaux et al., 2008a, 2008b). Elongin B/C proteins, originally identified as regulators of RNA polymerase II activity, directly interact with the SOCS box of SOCS proteins (Aso et al., 1995; Kamura et al., 1998). Interestingly, CIS interaction with phosphorylated tyrosine residues on various receptors is influenced by Elongin B/C interaction and this appears to be unique for CIS (Piessevaux et al., 2008a, 2008b). SOCS proteins, including CIS, are rapidly degraded via proteasome-dependent pathways, and ubiquitination of CIS has been observed in some systems (Lee et al., 2008; Piessevaux et al., 2008a, 2008b; Tauchi et al., 2001; Verdier et al., 1998).

Dopamine released from hypothalamic dopaminergic neurons inhibits pituitary PRL secretion. PRL normally functions in short-loop negative feedback to increase hypothalamic dopaminergic neuronal activity thereby decreasing pituitary PRL secretion (Arbogast and Voogt, 1991; Demarest et al., 1984). PRL signaling increases hypothalamic dopaminergic neuronal activity, tyrosine hydroxylase (TH) phosphorylation and activity, nuclear localization and phosphorylation of STAT5B (not STAT5A), and CIS mRNA levels (G. M. Anderson et al., 2006; S. T. Anderson et al., 2006; Arbogast, 2001; Arbogast and Voogt, 1997; Brown et al., 2012; Lerant et al., 2001; Ma et al., 2005; Yip et al., 2012). CIS appears to regulate PRL signaling in these neurons (G. M. Anderson et al., 2006; S. T. Anderson et al., 2006; Grattan et al., 2008). The negative feedback loop is inhibited during lactation and late pregnancy (Arbogast and Voogt, 1996; Demarest et al., 1983), potentially in part by increased CIS levels (G. M. Anderson et al., 2006; S. T. Anderson et al., 2006; Grattan et al.,

2008; Steyn et al., 2008). Given the apparent short half-life of CIS protein and the potential importance of CIS in regulating PRL responsiveness of hypothalamic dopaminergic neuronal activity, it is necessary to understand mechanisms regulating CIS protein stability.

Although CIS has been described as an ubiquitinated protein, the residues necessary for CIS ubiquitination and the influences of ubiquitination on CIS functional properties have not been investigated. Additionally, the relationship between CIS ubiquitination and CIS interactions with Elongin B/C and the E3 ubiquitin ligase complex have not been explored. In this study we sought to determine the specific CIS lysine residues responsible for CIS ubiquitination and whether CIS ubiquitination is dependent on interactions with the E3 ubiquitin ligase complex. We also examined the influence of ubiquitination and interaction with Elongin B/C proteins on CIS functional properties including protein stability and inhibition of PRLR-STAT5B signaling.

2. Materials and Methods

2.1 Cell line maintenance

HEK 293t (ATCC) cells were maintained in Dulbecco's modified Eagle's medium (DMEM) supplemented with 10% fetal bovine serum (FBS) and penicillin/streptomycin. Cath.a differentiated CAD cells (Qi et al., 1997) were maintained in DMEM:F-12 (1:1) medium supplemented with 8% FBS and penicillin/streptomycin. All cells were maintained in 37°C humidified incubator at 5% CO2.

2.2 DNA constructs

The rat PRLR and STAT5B cDNAs were generous gifts from Dr. Paul A. Kelly (INSERM, Paris, France) and Dr. Li-yuan Yu-Lee (Baylor College of Medicine, Houston, TX), respectively. Rat CIS was cloned from pituitary cDNA. A single C to T base pair difference at 559 of the coding region (compared to accession number NM 031804.1) was identified and corresponded to a serine to proline conversion at position 187. The translated protein sequence is similar to accession number AAC17502.1. This nucleotide difference was confirmed in CIS clones obtained from both rat ovary and pheochromocytoma PC12 cDNA. Rat SOCS3 (genomic accession number NW 047344.1), rat ubiquitin (accession number NM 017314.1) and Elongin C (accession number NM 001270563.1) were cloned by PCR from rat pituitary or rat PC-12 cDNA. Mouse CUL5 (accession number BC075710.1) was purchased from Open Biosystems (Thermo Scientific). PCR primers contained restriction endonuclease sites to allow for ligation or in-frame ligation into pcDNA3, N-terminal yellow fluorescent protein (YFP), N-terminal hemagglutinin (HA) epitope tag or N-terminal FLAG epitope tag CMV-driven expression vectors. The N-terminal HA epitope tag and N-terminal FLAG epitope tag CMV-driven expression vectors were generated in house and have a similar multiple cloning site as peGFP-N3. The rat casein promoter (−344bp to −1bp) was cloned from rat genomic DNA by PCR and ligated into pGL3 basic vector (Promega). Primers used to amplify open reading frames (ORF) or used for RT-PCR are listed in Table 1 (supplemental data). CIS lysine to arginine, Elongin B/C and Cul box (Piessevaux et al., 2008a, 2008b) mutations were generated by PCR. The constitutively active N642H STAT5B mutant (Ariyoshi et al., 2000) was also generated by PCR. Primers were designed that

contained the indicated amino acid substitutions and specific restriction endonuclease sites to facilitate subcloning. PCR products were digested with the appropriate restriction endonucleases and used to replace the corresponding region within the ORF. Glutathione S-transferase (GST)-CIS bacterial expression vectors were generated by subcloning CIS or the CIS mutants into PGEX2t vector (GE Healthcare). All ligation reactions were performed using ligase buffer (Invitrogen) and T4 ligase (New England BioLabs) and were incubated at room temperature. Ligation reactions were used to transform DH5α *E. coli*. Sequence identities for all constructs were verified by DNA sequencing on a Beckman Coulter CEQ 8000. Protein expression was carried out as previously described in DH5α *E. coli* (Jensik et al., 2004).

2.3 CAD PRLR-HA stable cell line

PRLR-HA stable CAD cells were generated by lentivirus transduction. A PRLR-HA cDNA was used to replace the GFP coding region in the pLJM1-EGFP (Sancak et al., 2008) lentiviral plasmid, which also contains a phosphoglycerate kinase promoter-driven puromycin resistance gene. HEK293t cells were transfected with pLJM1-PRLR-HA, pCMV-VSVG and pCMV-dR8.2 dvpr (Stewart et al., 2003) using the calcium phosphate technique. Medium was replaced 18 hrs after transfection. Lentiviral containing medium was collected 48 hrs later and centrifuged at 1000 × g for 10 minutes. Hexadimethrine bromide (Sigma) was added to the medium (final concentration 8 μg/mL) and the medium was used to infect CAD cells on 35 mm plates for 4 hrs. Medium on the CAD cells was replaced and 3 days later, PRLR-HA stable cells were selected using 4 μg/mL puromycin. Cells were maintained in CAD medium with puromycin. PRLR-HA expression was confirmed by RT-PCR and Western blot using primers for PRLR and anti-HA antibodies, respectively (Fig. 1A and 1B).

2.4 Chromatin immunoprecipitation (ChIP)

ChIPs were performed as previously described (Jensik and Arbogast, 2011). Briefly, stable PRLR-HA CAD cells were treated with vehicle or rPRL for 1 hr prior to cross-linking with formaldehyde. ChIP was performed using 1 μg Anti-STAT5B (Santa Cruz Biotechnology; G-2) or normal mouse immunoglobulin (mIgG; Santa Cruz Biotechnology). ChIP samples were analyzed by PCR using mouse *Cis* −184 and +4200 PCR primer sets (Basham et al., 2008). PCR products were separated on acrylamide gels and stained with ethidium bromide.

2.5 Western blot

PRLR-HA stable CAD cells on six well plates (150,000 cells/well) were treated with vehicle or PRL and DMSO or MG132 (CalBiochem) overnight. Collected cells were sonicated in co-immunoprecipitation (Co-IP) lysis buffer containing 150 mM sodium chloride, 50 mM Tris (pH=7.5), 1.0% Triton X-100, 1.0 mM EDTA, 1 mM sodium fluoride, 0.2 mM sodium orthovanadate, 10 μM MG132, aprotinin (10 μg/mL), leupeptin (10 μg/mL) and pepstatin (10 μg/mL). For transient transfection experiments, CAD and Hek293t cells were plated on six well plates (150,000 cells/well) and were transfected with 2.5 μg of indicated CIS expression vector. For MG132 experiments, medium was replaced 18 hrs after transfection and cells were treated overnight with 10 μM MG132. For cycloheximide (CHX) (Sigma)

experiments, 24 hrs after the medium change, cells were treated with 100 μg/mL CHX for the indicated times. To determine the influence of CIS or the various CIS mutants on phospho-STAT5 levels, cells were transfected with 1 μg PRLR and STAT5B (or 1 μg STAT5B-N642H) and 4 μg pcDNA3 or the indicated CIS constructs. Twenty-four hours after the medium change, cells were collected (N462H-transfected cells) or treated with vehicle or 1000 ng/mL rPRL for 30 minutes (PRLR/STAT5B-transfected cells) and then collected. Collected cells were sonicated in Co-IP lysis buffer. Lysates were separated on 7.5, 10 or 12 % SDS-PAGE gels and subjected to Western blot analysis as described previously (Liu and Arbogast, 2008) using anti-ubiquitin (mouse; 1:1000; Santa Cruz Biotechnology), anti-CIS (rabbit; 1:1000; Cell Signaling Technologies), anti-HA (mouse; 1:1000; Covance), anti-GFP (rabbit; 1:1000; Santa Cruz Biotechnology), anti-STAT5 (rabbit; 1:1000; Santa Cruz Biotechnology; C-17), anti-STAT5A (rabbit; 1:1000; Santa Cruz Biotechnology; L-20), anti-STAT5B (mouse; 1:1000; Santa Cruz Biotechnology; G-2), anti-tubulin (rabbit; 1:2500; Millipore) or anti-pSTAT5 (mouse; 1:2000; Invitrogen) antibodies.

2.6 Immunoprecipitations

PRLR-HA stable CAD cells on 100 mm dishes (1,000,000 cells/well) were treated overnight with PRL and 10 μM MG132. Collected cells were lysed in radioimmunoprecipitation assay (RIPA) buffer containing 150 mM sodium chloride, 50 mM Tris (pH=7.5), 1.0 % IGEPAL 630, 0.25% deoxycholate, 1 mM EDTA, 1 mM sodium fluoride, 0.2 mM sodium orthovanadate, 10 μM MG132, aprotinin (10 μg/mL), leupeptin (10 μg/mL) and pepstatin (10 μg/mL). Anti-ubiquitin antibodies or normal mouse IgG (1.0 μg) were preincubated with secondary sheep anti-mouse Dynabeads (Invitrogen) and then added to the lysates. For transient transfection experiments, cells were plated on 35 mm culture dishes and transfected with 2.5 μg FLAG- or HA- epitope tagged ubiquitin, CIS or SOCS3 constructs. Eighteen hours after transfection, medium was replaced and cells were treated overnight with 10 μM MG132. For naturing conditions, cells were collected and lysed (without sonication) in Co-IP lysis buffer (indicated earlier) containing 0.1% SDS for 30 min at room temperature. For denaturing conditions, collected cells were lysed in 100 μL Co-IP lysis buffer containing 1.0% SDS and heated at 95° C for 15 min. Samples were diluted with 900 μL lysis buffer without SDS for a final 0.1% SDS concentration. Lysates were cleared by centrifugation at 13,000 × g for 5 min at 4° C and applied to mouse anti-FLAG agarose beads (Sigma) overnight at 4° C. The beads were washed five times with lysis buffer and proteins were eluted from the agarose beads using Laemmli sample buffer with beta-mercaptoethanol. Immunoprecipitations were analyzed by Western blot using anti-HA (rabbit; 1:1000; Santa Cruz Biotechnology) and anti-FLAG (mouse 1:2000, Sigma) antibodies.

2.7 GST pulldown

HEK 293t cells were transfected with YFP-Elongin C or HA-CUL5 expression constructs. Thirty-six hours after transfection, cells were lysed in lysis buffer, cleared by centrifugation and incubated overnight at 4°C with GST or the indicated GST-CIS fusion proteins (~0.5 μg) attached to glutathione beads. Beads were washed extensively and proteins were eluted with Laemmli sample buffer. Eluted proteins were analyzed by Western blot using anti-GFP or anti-HA and anti-GST (mouse; 1:1000; Santa Cruz Biotechnology) antibodies.

2.8 Luciferase assay

Cells were plated at a density of 75,000 cells/ well on 24 well plates. Cells were transfected by the calcium phosphate method with 500 ng PRLR and 500 ng STAT5B (or 500 ng STAT5B N642H alone), 500 ng casein promoter, 2.5 ng CMV-Renilla luciferase (normalize transfection efficiency) and either 2 μg of indicated CIS mutant or pcDNA3 expression constructs. Eighteen hours after transfection, medium was replaced with serum-free medium containing 1% ITS universal culture supplement premix (BD Biosciences) for CAD cells or fresh medium for HEK 293t cells. Four hours later, cells were treated with vehicle (0.5% 0.1 M sodium bicarbonate buffer) or 1000 ng/mL rPRL (National Hormone and Pituitary Program) for 24 hrs. Luciferase assays were performed with the Promega Dual-Luciferase Reporter Assay System following manufacturer's protocol using a Bio-Tek Clarity dual injector luminometer.

2.9 Immunofluorescence

HEK 293t cells (150,000 cells/ 35 mm dish) were transfected with 0.5 μg peGFP-N3 and 1.0 μg pcDNA3, wt-CIS or CIS 6KR B/C constructs. Medium was replaced 18 hrs after transfection and 24 hrs later cells were fixed in 4% paraformaldehyde and permeabilized with 100% methanol. For immunofluorescence, cells were incubated with anti-CIS (rabbit; 1:1000; Cell Signaling Technologies) followed by Cy3-conjugated goat anti-rabbit IgG. DNA was stained with Hoescht dye 33258 (1 μg/mL). Cells were visualized with an Olympus BW50 fluorescence microscope using a 60× water objective.

2.10 Statistics

Data are expressed as mean ± SE of at least three independent experiments. Data were analyzed by one-way ANOVA followed by Fisher's multiple comparison post hoc test. P values less than 0.05 were considered significantly different.

3. Results

3.1 Characterization of stable PRLR-expressing TH-containing neuronal cell line

CIS regulates PRL signaling in a number of different cell types including dopaminergic neurons, and has been described as a rapidly degraded protein (Grattan et al., 2008; Piessevaux et al., 2008a, 2008b). Therefore, we first evaluated the regulation of endogenous CIS protein stability in a TH-expressing neuronal cell line. To confer PRL sensitivity, mouse catecholaminergic neuronal CAD cells were generated that stably express a C-terminal HA-tagged PRLR (PRLR-HA). RT-PCR and Western blot analysis were used to confirm stable expression of PRLR-HA in the stable CAD cells (Fig. 1A and 1B). These cells endogenously express TH, as shown by RT-PCR (Fig. 1A). As shown in the first two lanes of Fig. 1C, the PRLR-HA stable CAD cells also endogenously express both STAT5A and STAT5B proteins, as assessed by Western blot using antibodies specific for either the STAT5A or STAT5B isoform. Specificities of the STAT5A or STAT5B antibodies were confirmed using lysates from CAD cells transiently transfected with PRLR and either STAT5A or STAT5B (Fig. 1C). Note that 20 fold less protein quantity was loaded for the third and fourth lanes of blot in Fig. 1C, so endogenous STAT5 was not detected in lysates

from transiently transfected cells. PRL treatment increased pSTAT5 levels in both PRLR-HA stable CAD cells and CAD cells transiently transfected with PRLR and either STAT5A or STAT5B (Fig. 1C). PRL treatment also increased STAT5B recruitment to the previously characterized STAT5 response elements within the *Cis* promoter (−184) as determined by ChIP (Fig. 1D). Control regions downstream of the *Cis* promoter (+4200) did not show STAT5B recruitment. Taken together, PRL was able to activate the PRLR-STAT5B signaling pathway in these cells.

3.2 Inhibition of proteasomal degradation increased endogenous and over-expressed CIS levels

PRLR-HA stable CAD cells were then used to determine if endogenous CIS protein levels were regulated by proteasomal degradation. PRLR-HA stable CAD cells were treated with PRL and DMSO (vehicle) or the proteasome inhibitor MG132. Compared to vehicle-treated cells, MG132 increased CIS protein levels (Fig. 2A, top panel). Higher intensity scans indicated higher molecular CIS bands unique to the MG132 treatment group, which most likely indicate ubiquitin covalent attachment to CIS (Fig 2A, bottom panel). Endogenous ubiquitinated proteins were then immunoprecipitated from PRL- and MG132-treated PRLR-HA CAD stable cells using anti-ubiquitin antibodies or non-immune mIgG (control) followed by Western blots using anti-CIS or anti-ubiquitin antibodies (Fig. 2B). Ubiquitin-precipitated CIS (Fig. 2B, top panel) which indicated interactions between endogenous ubiquitin and CIS in the PRLR-HA stable CAD cells. As expected, ubiquitinated proteins were detected in both the input (first lane) and ubiquitin-precipitated (third lane) samples (Fig. 2B, bottom panel). As shown in the center lane of Fig. 2B, CIS and ubiquitin were not detected in the control non-immune mouse IgG immunoprecipitation.

We next determined if the regulation of CIS protein stability was similar in HEK293t and CAD cell lines transiently transfected with a CIS expression construct. CAD and HEK293t cells were co-transfected with GFP- and HA-tagged CIS or SOCS3 and treated with vehicle or MG132. MG132 was again able to markedly increase levels of CIS in both transfected cell lines (Fig. 2C and 2D, top panels). The MG132-mediated increase in CIS protein was similar to the increase observed in endogenous CIS protein in both CAD (Fig. 2C) and Hek293t (Fig. 2D) cells. SOCS3 protein levels also increased with MG132 treatment. However, SOCS3 appeared more stable in vehicle-treated HEK293t than CAD cells. The calculated molecular weights of HA-CIS and HA-SOCS3 are 31.0 and 27.2 kDa, respectively. The main form of CIS migrated slower than expected in SDS-PAGE gels. A similar migration pattern of epitope-tagged CIS relative to molecular weight standards has been demonstrated elsewhere (Ram and Waxman, 1999). Higher molecular weight CIS proteins were also apparent using higher intensity scans (Fig. 2C and 2D, bottom panels). The banding pattern was similar to endogenous CIS experiments (Fig. 2A).

3.3 CIS showed both covalent ubiquitin attachment and non-covalent interactions with ubiquitinated proteins

The rat CIS primary amino acid sequence contains six conserved lysine residues, at positions 59, 72, 98, 121, 188 and 208, that may act as substrates for ubiquitin conjugation. To determine whether CIS is ubiquitinated, all six lysine residues were first mutated to

arginine residues (6KR) to eliminate potential ubiquitin lysine conjugation sites on CIS. Cells were then transfected with FLAG-ubiquitin and HA-CIS, HA-6KR or HA-SOCS3 expression vectors and treated with MG132 (Figs. 3A and 3B). Anti-FLAG (ubiquitin) Co-IP experiments were performed to establish if CIS interacted with and/or was conjugated to ubiquitin. Co-IPs were followed by Western blot analysis using anti-HA (CIS) or anti-FLAG (ubiquitin) (Fig. 3A). As shown in the first lane, FLAG-ubiquitin precipitated the main form of CIS and also several higher molecular weight CIS bands (Fig. 3A, top panel). As shown in the second lane, FLAG-ubiquitin precipitated the main form of 6KR, however no higher molecular weight CIS bands were present. As shown in the third lane, FLAG-ubiquitin also precipitated the main form of SOCS3 and a number of higher molecular weight forms of SOCS3. The main forms of CIS and SOCS3 were observed in lysates used as inputs for the immunoprecipitations (Fig. 3B, top panel). Numerous ubiquitinated proteins, especially in the higher molecular weight range, were precipitated with anti-FLAG (ubiquitin) (Fig. 3A, bottom panel) and were also observed in input lysates without immunoprecipitation (Fig. 3B, bottom panel).

Epitope tags were then switched and cells were transfected with FLAG-CIS and HA-ubiquitin and treated with MG132 (Figs. 3C and 3D). Control transfections were also performed using HA-CIS (instead of FLAG-CIS) with HA-ubiquitin to demonstrate anti-FLAG antibody specificity. As shown in the first lane of the blots in Fig 3C, FLAG-CIS immunoprecipitations with anti-FLAG showed a range of HA-ubiquitin higher molecular weight proteins (Fig. 3C, top panel), in addition to those recognized by the FLAG antibody for CIS (Fig. 3C, bottom panel). Although the range of ubiquitinated proteins detected with anti-HA for ubiquitin (Fig. 3C, top panel) was not apparent for FLAG-CIS, there were higher molecular weight CIS proteins (Fig. 3C, bottom panel) similar to those observed in the FLAG-ubiquitin with HA-CIS immunoprecipitation (Fig. 3A, top panel). As shown in the second lane of the blots in Fig. 3C, FLAG immunoprecipitations showed no CIS (bottom panel) or ubiquitin (top panel) proteins in the negative control experiments, in which cells were transfected with HA-CIS and HA-ubiquitin. FLAG-CIS, but not HA-CIS was identified in the input lysate with anti-FLAG, indicating specificity of epitope tag antibodies (Fig. 3D, top panel). Numerous HA-tagged ubiquitinated proteins were observed in the input lysates (Fig. 3D, bottom panel). The main form of HA-CIS was also detected in lysates of cells transfected with HA-CIS, as shown in the second lane of Fig. 3D (bottom panel). Combined these data indicate CIS interacts with other ubiquitinated proteins and is a substrate for ubiquitin conjugation. There is also an apparent difference between the abundance and degree of CIS ubiquitination compared to SOCS3 ubiquitination (Fig. 3A, top panel).

The interaction between ubiquitin and CIS was further characterized by using denaturing and naturing conditions to determine CIS and ubiquitin covalent and non-covalent interactions. These experiments also included the CIS 6KR mutant. Cells were transfected with FLAG-ubiquitin and either HA-CIS or the HA-6KR mutant. A control transfection was performed using HA-ubiquitin instead of FLAG-ubiquitin. For denaturing conditions, collected cells were lysed in lysis buffer containing 1.0% SDS and heated to eliminate non-covalent ubquitin-CIS interactions. Covalent ubiquitin interactions should remain intact. Samples were diluted with lysis buffer without SDS for a final 0.1% SDS concentration

prior to immunoprecipitation. For naturing conditions, collected cells were lysed in lysis buffer containing 0.1% SDS. Covalent and non-covalent ubiquitin interactions should remain intact in these lysates. Immunoprecipitations of denatured and natured lysates were then performed under identical conditions with anti-FLAG (ubiquitin) conjugated to agarose. Under naturing conditions depicted in the second and fourth lanes of the blot in Fig. 4A, the main form of CIS for both wt and the 6KR mutant, respectively, co-immunoprecipitated with FLAG-ubiquitin. Denaturing conditions markedly decreased the amount of the main form of CIS detected on the HA immunoblot, as shown in the first and third lanes of the blot in Fig. 4A. There was no reduction in the amount of immunoprecipitated FLAG-ubiquitin as detected on the FLAG immunoblot (Fig. 4C). These data suggest non-covalent interactions of ubiquitin with the main form of both wt CIS and CIS 6KR mutant. Higher molecular weight ubiquitinated CIS proteins were apparent in both the naturing and denaturing samples for wt-CIS. An increased intensity scan (Fig. 4B) indicates higher molecular weight CIS proteins in the first and second lanes of the blot that were not visible in the lower intensity scan (Fig. 4A). These higher molecular weight CIS proteins were not present in the third and fourth lanes for the CIS 6KR mutant (Fig. 4B), suggesting ubiquitin covalent interactions with only wt CIS. The control immunoprecipitation in which the FLAG on ubiquitin was replaced with HA showed no anti-FLAG immunoprecipitation of either CIS or ubiquitin (Figs. 4A – 4C, fifth lane). Numerous other immunoprecipitated FLAG-tagged ubiquitinated proteins were similarly observed with anti-FLAG in cells transfected with HA-CIS or HA-6KR shown in lanes 1–4, but not HA-ubiquitin shown in lane 5 (Fig. 4C). CIS main form was detected in input lysates from all cells transfected with HA-CIS or HA-6KR (Fig. 4D). These data support that CIS has covalent and non-covalent interactions with ubiquitin.

3.4 CIS is ubiquitinated on each lysine residue

To determine which CIS lysine residue is necessary for ubiquitin attachment, each of the six CIS lysine residues was individually mutated to an arginine residues leaving the other five lysine residues unchanged. FLAG-ubiquitin was co-expressed with HA-tagged CIS, single lysine to arginine CIS mutants or CIS 6KR mutant. FLAG-ubiquitin was immunoprecipitated from the cells and the immunoprecipitants were analyzed by Western blot for HA-CIS using anti-HA (Fig. 5A, top panel). As shown in the first lane of the top panel, wt-CIS again showed higher molecular weight bands above the main form (Fig. 5A). Higher molecular bands were also visible for each of the single lysine to arginine CIS mutants, indicating multiple lysines are ubiquitinated. As shown in the last lane, mutation of all six lysines in 6KR construct eliminated the higher molecular weight bands. CIS constructs were then generated that mutated five of the six lysine residues to arginine residues leaving only a single lysine residue for each CIS mutant. Similar Co-IP experiments were performed on these mutants (Fig. 5B). In addition to the higher molecular weight bands apparent for wt CIS in the first lane, higher molecular bands above the main form of CIS mutants were also apparent for K59, K72, K98, K188, and K208 CIS and the higher molecular weight forms were weakly present for K121 CIS (Fig. 5B, top panel). Multiple bands above the main form for the CIS mutants containing a single lysine residue likely indicate potential mono-, di- and poly-ubiquitin attachments. There appears to be a reduction in the intensity of the higher molecular weight CIS proteins when K188 and possibly K72

are mutated (Fig 5A, top panel) and a slight increase when K188 is the only lysine remaining (Fig 5B, top panel). Similar results were also observed in CAD cells (data not shown). Numerous ubiquitinated proteins were similarly observed with each of the CIS mutants in immunoblots using anti-FLAG (ubiquitin) antibody (Fig. 5A and 5B, bottom panels). These data indicate that all six CIS lysine residues are potential substrates for ubiquitin attachment, although there may be a preference for specific lysines, notably K188 or K72.

3.5 Elongin B/C interactions are not necessary for CIS ubiquitination

Given that CIS also functions in an E3 ubiquitin ligase complex through the B/C box, we next evaluated whether Elongin B/C interactions were necessary for CIS ubiquitination. The CIS Elongin B/C box was mutated to eliminate Elongin B/C interactions in both wt-CIS and CIS 6KR mutant (B/C and 6KR B/C, respectively). To confirm the B/C box mutation and determine whether mutation of the lysine residues disrupted interactions with Elongin C and CUL5 proteins, GST fusion proteins were generated for CIS, 6KR, B/C and 6KR B/C and used in GST pulldowns with lysates from HEK293t cells transfected with YFP-Elongin C or HA-CUL5. The purity and relative amounts of the GST, GST-CIS and GST-CIS mutant fusion proteins are shown on the GST immunoblot (Fig. 6A, bottom panel). Elongin C (Fig. 6A, top panel) and CUL5 (Fig. 6B) interacted with CIS and the 6KR mutant shown in second and third lanes of blot, respectively, but not with either the B/C or 6KR B/C mutants, shown in fourth and fifth lanes of blots, respectively. Control experiment shown in the first lane using GST alone showed no interaction with Elongin C or CUL5 proteins (Fig. 6A).

Co-IP experiments from cells transfected with FLAG-ubiquitin and HA-CIS, 6KR, B/C or 6KR B/C expression constructs were then performed to determine if Elongin B/C interactions influence CIS ubiquitination. Western blot analysis indicated that mutation of the Elongin B/C interaction (B/C) did not inhibit CIS ubiquitination, as evidenced by the higher molecular forms of CIS for the B/C mutant shown in the third lane (Fig. 6C). Mutation of the lysine residues inhibited CIS ubiquitination in both the 6KR and the 6KR B/C mutants, shown in the second and fourth lanes, respectively, indicating CIS ubiquitination is independent of Elongin B/C and CUL5 interactions.

3.6 Ubiquitin and Elongin B/C interaction on CIS degradation rates

To determine the influence of ubiquitination and Elongin B/C interaction on CIS protein stability, cells were co-transfected with GFP and wt, 6KR, B/C or 6KR B/C CIS constructs. Western blots were performed on cell lysates to determine the expression levels of the various CIS proteins after normalization to GFP levels (Fig. 7A). The B/C mutant had similar expression levels compared to wt-CIS. The 6KR mutant had significantly increased expression (3.1-fold) compared to wt-CIS and the 6KR B/C mutant showed significantly increased expression (4.8-fold) compared to both wt-CIS and the 6KR mutant. Similar results were observed in CAD cells (supplemental Fig. 1)

The effects of the various CIS mutations on CIS protein stability were determined by comparing CIS expression levels in vehicle-treated to MG132-treated cells (Fig. 7B). A CIS Cul box mutation was also tested in this assay. CIS protein levels for each treatment were

first normalized to co-transfected GFP levels. The percentage of vehicle to MG132 CIS levels was determined for each mutant. Wt-CIS showed 5.9% stability. The B/C and Cul mutants had similar stabilities to wt-CIS. The 6KR and 6KR Cul mutants showed significantly increased stability, but the most marked stability was observed with the 6KR B/C mutant. Interestingly, 6KR B/C mutant stability was still sensitive to MG132 treatment, in spite of the fact that CIS ubiquitination sites were missing and the ability to form a complex with E3 ubiquitin ligase was absent.

Cells transfected with wt-CIS, 6KR, B/C or 6KR B/C constructs were then treated with CHX for 2 or 4 hrs to determine the influences of CIS ubiquitination and Elongin B/C interaction on CIS degradation rates (Fig. 7C). The B/C mutant had a similar degradation profile as wt-CIS at both 2 and 4 hrs. The 6KR mutant protein showed decreased degradation at 2 and 4 hrs compared to wt-CIS. The decline in degradation was most marked with the 6KR B/C mutant being significantly less than both wt-CIS and the 6KR mutant at 2 and 4 hrs, suggesting both CIS ubiquitination and interaction with Elongin B/C play a role in CIS protein degradation. However, it is notable that inhibition of CIS ubiquitination and interaction with Elongin B/C were not sufficient to completely prevent CIS degradation.

3.7 Ubiquitin and Elongin B/C interactions on CIS-mediated inhibition of PRLR signaling

The effects of lysine mutations and Elongin B/C interactions on CIS-mediated inhibition of PRLR-STAT5B signaling were investigated. CAD and HEK 293t cells were transfected with PRLR, STAT5B and casein promoter-luciferase reporter together with pcDNA3, wt-CIS, 6KR, B/C or 6KR B/C expression constructs at a 4:1 ratio of CIS to PRLR. SOCS3 expression constructs were also used, but at a 1:1 ratio. Compared to vehicle-treated cells, 24 hr PRL treatment increased casein promoter activity in CAD and HEK 293t cells co-transfected with pcDNA3 by 10.1- and 115-fold, respectively (Fig. 8A and 8E). wt CIS and the 6KR mutant inhibited casein promoter activities in both cell lines to around 50% of the pcDNA3-transfected, PRL-treated group (Fig. 8B and 8F). Compared to wt-CIS, the B/C and 6KR B/C mutants had significantly reduced inhibition of casein promoter activity at around 70% and 75% in CAD and HEK293t cells, respectively. SOCS3 co-expression completely suppressed PRLR-mediated increases in casein promoter activity (Fig. 8B and 8F). Expression levels of STAT5, CIS, and SOCS3 proteins in luciferase assay lysates were also determined by Western blot using antibodies for STAT5, HA (CIS, 6KR, B/C, 6KR B/C and SOCS3), and tubulin (Fig. 8C and 8G). STAT5 expression was similar in all groups. JAK2 mRNA was detected in both HEK293t and CAD cells (supplemental Fig. 2).

Western blot analyses of cells co-transfected with PRLR and STAT5B together with pcDNA3 or the various CIS constructs were performed to determine the influence of CIS or the various CIS mutants on pSTAT5 levels (Fig. 8D and 8H). In both cell lines, PRL treatment for 30 min caused a marked increase in pSTAT5 levels in pcDNA3-transfected control cells when compared to vehicle treatment, as shown comparing the first and second lanes of the blots. Co-expression of wt-CIS or the 6KR mutant caused similar decreases in pSTAT5 levels, as shown in third and fourth lanes of the blots. In contrast, higher levels of pSTAT5 were observed with co-expression of either the B/C or 6KR B/C mutant when compared to levels with wt-CIS or the 6KR mutant as shown in the fifth and sixth lanes of

the blots. Nearly undetectable levels of pSTAT5 were observed with SOCS3 co-expression in the last lanes. These data suggest that B/C Elongin interaction plays a role in CIS inhibitory actions on PRLR signaling.

Given the B/C mutation seemed to attenuate CIS inhibitory actions on PRLR-STAT5B signaling, we set out to explore the ability of CIS and the various CIS mutants to inhibit transcriptional activity and phosphorylation of a constitutively active form of STAT5B-N642H. STAT5B-N642H is phosphorylated and transcriptionally active in the absence of cytokine receptor activation (Ariyoshi et al., 2000). CIS inhibitory actions on STAT5B-N642H may indicate other mechanisms of CIS-mediated inhibition downstream of cytokine receptors. HEK 293t cells were co-transfected with a casein promoter-luciferase reporter construct and wt-STAT5B or the N642H mutant together with pcDNA3, CIS, 6KR, B/C or 6KR B/C constructs at a 4:1 CIS:STAT5B ratio. Compared to wt-STAT5B at basal activation levels, the N642H mutant showed a 29.5-fold increase in casein promoter activity (Fig. 9A). wt CIS was able to inhibit the N642H-mediated activation of casein promoter activity to around 60% (Fig. 9B). The 6KR and B/C mutants showed similar levels of inhibition to wt-CIS. However, the 6KR B/C mutant displayed significantly greater inhibition than wtCIS or other CIS mutants to 35.8%. Expression levels of STAT5, N642H and CIS relative to tubulin proteins in luciferase assay lysates were also determined by Western blot using antibodies for STAT5 (STAT5 and N642H mutant), HA tag (CIS, 6KR, B/C and 6KR B/C) or tubulin. (Fig. 9C). STAT5 (wt and N642H) expression was similar with CIS or SOCS3 co-transfection. Western blots were also performed on similarly transfected cells to determine the influence of CIS or the CIS mutants on pSTAT5 levels (Fig. 9D). The levels of pSTAT5 were decreased in all cells co-transfected with CIS or the various CIS mutants.

Cells were then transfected with GFP and pcDNA3, wt or 6KR B/C CIS constructs without epitope tags. GFP was used to label transfected cells and CIS localization was determined by immunofluorescence using anti-CIS (Fig. 9E). As shown in the top panels, wt-CIS showed strong cytoplasmic localization and the 6KR B/C mutant showed both nuclear and cytoplasmic localization. CIS immunofluorescence was not detected in the control pcDNA3-transfected cells

4. Discussion

We are reporting ubiquitination of endogenous CIS in a PRLR-expressing stable TH-containing CAD neuronal cell line. Similar to endogenous CIS, CIS ubiquitination was observed with FLAG- or HA-tagged CIS transiently transfected into CAD and HEK293t cells. Our results indicate that each of the six lysine residues in CIS can serve as sites for ubiquitin attachment, although the efficiency of ubiquitination may differ between specific lysines. CIS protein interacted with Elongin C and CUL5 proteins of the E3 ubiquitin ligase complex, but CIS ubiquitination was not dependent on CIS interaction with Elongin B/C proteins. CIS ubiquitination and CIS interactions with Elongin B/C modulated functional properties of the CIS protein. Both CIS ubiquitination and CIS interactions with Elongin B/C had a role in CIS protein stability. CIS interactions with Elongin B/C complex

influenced CIS modulation of PRLR signaling pathways, but this interaction was not solely responsible for CIS ability to suppress PRLR signaling in either CAD or HEK293t cells.

Previous studies indicate that CIS is ubiquitinated as shown by multiple CIS protein bands and through ubiquitin Co-IP experiments (Tauchi et al., 2001; Verdier et al., 1998). In this study, we show that each of the CIS lysine residues is a substrate for ubiquitin attachment. High molecular weight polyubiquitinated proteins usually observed for many other ubiquitinated proteins were not readily apparent for CIS. This may indicate distinct ubiquitin attachment to CIS. CIS has been described as a monoubiquitinated protein (Krebs and Hilton, 2000; Landsman and Waxman, 2005). However our study indicates that each of the lysine residues can have more than one ubiquitin linkage as indicated by multiple higher molecular weight ubiquitin-containing bands for CIS. Immunoprecipitations using reversal of epitope tags and denaturing conditions also uncovered non-covalent associations of ubiquitin with CIS, notably with the main form of CIS. These non-covalent interactions likely result from CIS being linked to the E3 ubiquitin ligase complex through its interactions with Elongin B/C and CUL proteins. Interestingly, CIS ubiquitination was not dependent on Elongin B/C interactions and therefore other mechanisms beyond CIS involvement in the E3 ubiquitin ligase complex target CIS for ubiquitination.

Inhibition of CIS ubiquitination by mutation of the lysine residues increased CIS protein stability. As shown here and elsewhere (Piessevaux et al., 2008a, 2008b), mutation of the Elongin B/C box had no effect on CIS stability. However, co-mutation of the Elongin B/C interaction and inhibition of ubiquitination (6KR B/C) enhanced CIS stability above that observed with loss of ubiquitination sites. These data indicate that a primary mechanism for CIS degradation was through CIS ubiquitination. In the absence of ubiquitination, interaction with Elongin B/C can contribute to CIS degradation. Counter-intuitively, Elongin B/C proteins appear to stabilize CIS (Haan et al., 2003; Piessevaux et al., 2008a, 2008b). For the proteins forming the E3 ubiquitin ligase complex, this property seems to be unique to Elongin B/C. Mutation of the Cul Box either alone or combined with mutation of CIS lysines had no influence on CIS levels. This could mean that Elongin B/C proteins can influence CIS stability separately from the interaction with CUL proteins and the E3 ligase complex. Even with mutation of both the lysine residues and the Elongin B/C interaction, CIS protein still showed degradation, suggesting that CIS is degraded by mechanisms other than direct ubiquitination and involvement in the E3 ubiquitin ligase. Other regions of CIS may interact with other proteins that are targeted for degradation. SOCS1 degradation can be influenced by interactions with the tripartite motif TRIM8/GERP protein (Toniato et al., 2002). Also phosphorylation appears to regulate SOCS turnover rates (Chen et al., 2002; Haan et al., 2003).

A functional consequence of increased CIS expression is inhibition of the PRLR signaling pathway (Kile and Alexander, 2001). Mutation of the Elongin B/C box in the SOCS box of CIS impeded its ability to suppress STAT5B phosphorylation and casein promoter activation, indicating that CIS inhibition of PRLR signaling was dependent on interaction with Elongin B/C. In contrast, CIS ubiquitination status had no influence on CIS inhibition of PRLR signaling. These data suggest that the mechanism for CIS inhibition of PRLR signaling is similar to other cytokine receptors. Elongin B/C interactions influence CIS

interaction with phosphotyrosine residues from erythropoietin, interleukin and growth hormone receptors (Piessevaux et al., 2008a, 2008b). Given the similarities between growth hormone receptor and PRLR, B/C interactions likely influence CIS binding to phosphotyrosine residues on the PRLR. It is noteworthy that mutation of the Elongin B/C box only partially prevented the CIS inhibitory effects on PRLR signaling and that other mechanism(s) may also contribute to CIS action.

CIS inhibited the constitutively active form of STAT5B-N642H. The mechanisms underlying the constitutive phosphorylation and activation of STAT5B-N642H in the absence of cytokine activation remain unclear (Ariyoshi et al., 2000). These data indicate that CIS has potential inhibitory actions downstream of CIS-PRLR receptor interactions. The CIS 6KR B/C mutant showed both increased inhibition of STAT5B-N642H activity and nuclear localization compared to wt-CIS, which may imply potential nuclear functions for CIS. MG132 treatment was previously shown to increase CIS and SOCS nuclear accumulation (Lee et al., 2008). This localization profile was thought to occur because of the increased CIS level (Lee et al., 2008). *In vivo*, CIS may also show nuclear localization under certain endocrine conditions, as demonstrated in hypothalamic dopaminergic neurons during lactation (S. T. Anderson et al., 2006). Prolactin treatment increases CIS levels in both the cytoplasm and nucleus in the hypothalamus of rats. Further work is needed to identify potential functions of nuclear CIS and also the mechanism by which CIS can inhibit the constitutively active form of STAT5B.

CIS appears to have both short and long term effects on cytokine sensitivity of specific tissues during certain physiological states. During pregnancy, the mouse liver shows diminished growth hormone responsiveness, which has been attributed to increased CIS levels (Miquet et al., 2004). CIS levels are also elevated in mammary tissue and ovaries during the second half of pregnancy in the mouse (Anderson et al., 2009; Tonko-Geymayer et al., 2002) potentially indicating modulatory functions of CIS on cytokine signaling in these tissues. CIS mRNA is increased in the hypothalamus of lactating rats and may act in part to decrease the responsiveness of dopaminergic neurons to PRL (G. M. Anderson et al., 2006; S. T. Anderson et al., 2006). Transgenic mice over-expressing CIS show impaired growth and mammary gland development possibly due to inhibition of growth hormone and PRLR signaling (Matsumoto et al., 1999). Mice deficient in CIS show alterations in interleukin signaling and spontaneously develop pulmonary disease (Yang et al., 2013).

In summary, CIS ubiquitination occurs separately from CIS interaction with the Elongin B/C E3 ubiquitin ligase complex. There also appears to be a complex relationship between CIS stability, function, ubiquitination and the interaction with Elongin B/C proteins.

Supplementary Material

Refer to Web version on PubMed Central for supplementary material.

Acknowledgements

We thank Dr. Paul A. Kelly (INSERM, Paris, France) and Dr. Li-yuan Yu-Lee (Baylor College of Medicine, Houston, TX) for rat PRLR and STAT5B cDNAs, respectively. We also thank Dr James T. K. Wang, Tufts

University (Boston, MA, USA) for providing us with CAD cells and Dr. A.F. Parlow (National Hormone & Peptide Program, Torrence, CA) for rPRL.

This work was supported by NIH grants HD045805 and HD048925. The content of the manuscript is the responsibility of the authors. The NIH had no involvement in study design, data collection, analysis and interpretation, decision to publish or preparation of the manuscript.

Abbreviations

CAD	Cath.a derived
CIS	cytokine-inducible SH2-containing protein
CHX	cycloheximide
ORF	open reading frame
PRL	prolactin
PRLR	prolactin receptor
STAT5	signal transducer and activator of transcription 5
SOCS	suppressors of cytokine signaling
TH	tyrosine hydroxylase

References

Anderson GM, Beijer P, Bang AS, Fenwick MA, Bunn SJ, Grattan DR. Suppression of prolactin-induced signal transducer and activator of transcription 5b signaling and induction of suppressors of cytokine signaling messenger ribonucleic acid in the hypothalamic arcuate nucleus of the rat during late pregnancy and lactation. Endocrinology. 2006; 147:4996–5005. [PubMed: 16857756]

Anderson ST, Barclay JL, Fanning KJ, Kusters DH, Waters MJ, Curlewis JD. Mechanisms underlying the diminished sensitivity to prolactin negative feedback during lactation: reduced STAT5 signaling and up-regulation of cytokine-inducible SH2 domain-containing protein (CIS) expression in tuberoinfundibular dopaminergic neurons. Endocrinology. 2006; 147:1195–1202. [PubMed: 16357045]

Anderson ST, Isa NN, Barclay JL, Waters MJ, Curlewis JD. Maximal expression of suppressors of cytokine signaling in the rat ovary occurs in late pregnancy. Reproduction. 2009; 138:537–544. [PubMed: 19502454]

Arbogast LA. Calmodulin and a cyclic nucleotide-dependent protein kinase facilitate the prolactin-induced increase in tyrosine hydroxylase activity in tuberoinfundibular dopaminergic neurons. Endocrine. 2001; 16:105–112. [PubMed: 11887930]

Arbogast LA, Voogt JL. Prolactin (PLR) receptors are colocalized in dopaminergic neurons in fetal hypothalamic cell cultures: Effect of PRL on tyrosine hydroxylase activity. Endocrinology. 1997; 138:3016–3023. [PubMed: 9202247]

Arbogast LA, Voogt JL. Hyperprolactinemia increases and hypoprolactinemia decreases tyrosine hydroxylase messenger ribonucleic acid levels in the arcuate nuclei, but not the substantia nigra or zona incerta. Endocrinology. 1991; 128:997–1005. [PubMed: 1703487]

Arbogast LA, Voogt JL. The responsiveness of tuberoinfundibular dopaminergic neurons to prolactin feedback is diminished between early lactation and midlactation in the rat. Endocrinology. 1996; 137:47–54. [PubMed: 8536641]

Ariyoshi K, Nosaka T, Yamada K, Onishi M, Oka Y, Miyajima A, Kitamura T. Constitutive activation of STAT5 by a point mutation in the SH2 domain. J Biol Chem. 2000; 275:24407–24413. [PubMed: 10823841]

Aso T, Lane WS, Conaway JW, Conaway RC. Elongin (SIII): a multisubunit regulator of elongation by RNA polymerase II. Science. 1995; 269:1439–1443. [PubMed: 7660129]

Babon JJ, Sabo JK, Soetopo A, Yao S, Bailey MF, Zhang JG, Nicola NA, Norton RS. The SOCS box domain of SOCS3: structure and interaction with the elonginBC-cullin5 ubiquitin ligase. J Mol Biol. 2008; 381:928–940. [PubMed: 18590740]

Basham B, Sathe M, Grein J, McClanahan T, D'Andrea A, Lees E, Rascle A. In vivo identification of novel STAT5 target genes. Nucleic Acids Res. 2008; 36:3802–3818. [PubMed: 18492722]

Brown RS, Piet R, Herbison AE, Grattan DR. Differential actions of prolactin on electrical activity and intracellular signal transduction in hypothalamic neurons. Endocrinology. 2012; 153:2375–2384. [PubMed: 22416085]

Chen XP, Losman JA, Cowan S, Donahue E, Fay S, Vuong BQ, Nawijn MC, Capece D, Cohan VL, Rothman P. Pim serine/threonine kinases regulate the stability of Socs-1 protein. Proc Natl Acad Sci U S A. 2002; 99:2175–2180. [PubMed: 11854514]

Demarest KT, McKay DW, Riegle GD, Moore KE. Biochemical indices of tuberoinfundibular dopaminergic neuronal activity during lactation: a lack of response to prolactin. Neuroendocrinology. 1983; 36:130–137. [PubMed: 6682185]

Demarest KT, Riegle GD, Moore KE. Prolactin-induced activation of tuberoinfundibular dopaminergic neurons: evidence for both a rapid 'tonic' and a delayed 'induction' component. Neuroendocrinology. 1984; 38:467–475. [PubMed: 6738811]

Dif F, Saunier E, Demeneix B, Kelly PA, Edery M. Cytokine-inducible SH2-containing protein suppresses PRL signaling by binding the PRL receptor. Endocrinology. 2001; 142:5286–5293. [PubMed: 11713228]

Endo T, Sasaki A, Minoguchi M, Joo A, Yoshimura A. CIS1 interacts with the Y532 of the prolactin receptor and suppresses prolactin-dependent STAT5 activation. J Biochem. 2003; 133:109–113. [PubMed: 12761205]

Grattan DR, Steyn FJ, Kokay IC, Anderson GM, Bunn SJ. Pregnancy-induced adaptation in the neuroendocrine control of prolactin secretion. J Neuroendocrinol. 2008; 20:497–507. [PubMed: 18266946]

Haan S, Ferguson P, Sommer U, Hiremath M, McVicar DW, Heinrich PC, Johnston JA, Cacalano NA. Tyrosine phosphorylation disrupts elongin interaction and accelerates SOCS3 degradation. J Biol Chem. 2003; 278:31972–31979. [PubMed: 12783885]

Hiltoc DJ, Richardson RT, Alexander WS, Viney EM, Willson TA, Sprigg NS, Starr R, Nicholson SE, Metcalf D, Nicola NA. Twenty proteins containing a C-terminal SOCS box form five structural classes. Proc Natl Acad Sci U S A. 1998; 95:114–119. [PubMed: 9419338]

Jensik PJ, Arbogast LA. Differential and interactive effects of ligand-bound progesterone receptor a and B isoforms on tyrosine hydroxylase promoter activity. J Neuroendocrinol. 2011; 23:915–925. [PubMed: 21815951]

Jensik PJ, Huggenvik JI, Collard MW. Identification of a nuclear export signal and protein interaction domains in deformed epidermal autoregulatory factor-1 (DEAF-1). J Biol Chem. 2004; 279:32692–32699. [PubMed: 15161925]

Kamizono S, Hanada T, Yasukawa H, Minoguchi S, Kato R, Minoguchi M, Hattori K, Hatakeyama S, Yada M, Morita S, Kitamura T, Kato H, Nakayama K, Yoshimura A. The SOCS box of SOCS-1 accelerates ubiquitin-dependent proteolysis of TEL-JAK2. J Biol Chem. 2001; 276:12530–12538. [PubMed: 11278610]

Kamura T, Maenaka K, Kotoshiba S, Matsumoto M, Kohda D, Conaway RC, Conaway JW, Nakayama KI. VHL-box and SOCS-box domains determine binding specificity for Cul2-Rbx1 and Cul5-Rbx2 modules of ubiquitin ligases. Genes Dev. 2004; 18:3055–3065. [PubMed: 15601820]

Kamura T, Sato S, Haque D, Liu L, Kaelin WG Jr, Conaway RC, Conaway JW. The Elongin BC complex interacts with the conserved SOCS-box motif present in members of the SOCS, ras, WD-40 repeat, and ankyrin repeat families. Genes Dev. 1998; 12:3872–3881. [PubMed: 9869640]

Kile BT, Alexander WS. The suppressors of cytokine signalling (SOCS). Cell Mol Life Sci. 2001; 58:1627–1635. [PubMed: 11706989]

Krebs DL, Hilton DJ. SOCS: physiological suppressors of cytokine signaling. J Cell Sci. 2000; 113(Pt 16):2813–2819. [PubMed: 10910765]

Landsman T, Waxman DJ. Role of the cytokine-induced SH2 domain-containing protein CIS in growth hormone receptor internalization. J Biol Chem. 2005; 280:37471–37480. [PubMed: 16154995]

Lee KH, Moon KJ, Kim HS, Yoo BC, Park S, Lee H, Kwon S, Lee ES, Yoon S. Increased cytoplasmic levels of CIS, SOCS1, SOCS2, or SOCS3 are required for nuclear translocation. FEBS Lett. 2008; 582:2319–2324. [PubMed: 18538139]

Lerant A, Kanyicska B, Freeman ME. Nuclear translocation of STAT5 and increased expression of Fos related antigens (FRAs) in hypothalamic dopaminergic neurons after prolactin administration. Brain Res. 2001; 904:259–269. [PubMed: 11406124]

Liu B, Arbogast LA. Phosphorylation state of tyrosine hydroxylase in the stalk-median eminence is decreased by progesterone in cycling female rats. Endocrinology. 2008; 149:1462–1469. [PubMed: 18096660]

Ma FY, Anderson GM, Gunn TD, Goffin V, Grattan DR, Bunn SJ. Prolactin specifically activates signal transducer and activator of transcription 5b in neuroendocrine dopaminergic neurons. Endocrinology. 2005; 146:5112–5119. [PubMed: 16123156]

Masuhara M, Sakamoto H, Matsumoto A, Suzuki R, Yasukawa H, Mitsui K, Wakioka T, Tanimura S, Sasaki A, Misawa H, Yokouchi M, Ohtsubo M, Yoshimura A. Cloning and characterization of novel CIS family genes. Biochem Biophys Res Commun. 1997; 239:439–436. [PubMed: 9344848]

Matsumoto A, Masuhara M, Mitsui K, Yokouchi M, Ohtsubo M, Misawa H, Miyajima A, Yoshimura A. CIS, a cytokine inducible SH2 protein, is a target of the JAK-STAT5 pathway and modulates STAT5 activation. Blood. 1997; 89:3148–3154. [PubMed: 9129017]

Matsumoto A, Seki Y, Kubo M, Ohtsuka S, Suzuki A, Hayashi I, Tsuji K, Nakahata T, Okabe M, Yamada S, Yoshimura A. Suppression of STAT5 functions in liver, mammary glands, and T cells in cytokine-inducible SH2-containing protein 1 transgenic mice. Mol Cell Biol. 1999; 19:6396–6407. [PubMed: 10454585]

Mayr S, Welte T, Windegger M, Lechner J, May P, Heinrich PC, Horn F, Doppler W. Selective coupling of STAT factors to the mouse prolactin receptor. Eur J Biochem. 1998; 258:784–793. [PubMed: 9874248]

Miquet JG, Sotelo AI, Bartke A, Turyn D. Suppression of growth hormone (GH) Janus tyrosine kinase 2/signal transducer and activator of transcription 5 signaling pathway in transgenic mice overexpressing bovine GH. Endocrinology. 2004; 145:2824–2832. [PubMed: 15016718]

Pezet A, Favre H, Kelly PA, Edery M. Inhibition and restoration of prolactin signal transduction by suppressors of cytokine signaling. J Biol Chem. 1999; 274:24497–24502. [PubMed: 10455112]

Piessevaux J, De Ceuninck L, Catteeuw D, Peelman F, Tavernier J. Elongin B/C recruitment regulates substrate binding by CIS. J Biol Chem. 2008a; 283:21334–21346. [PubMed: 18508766]

Piessevaux J, Lavens D, Peelman F, Tavernier J. The many faces of the SOCS box. Cytokine Growth Factor Rev. 2008b; 19:371–381. [PubMed: 18948053]

Qi Y, Wang JK, McMillian M, Chikaraishi DM. Characterization of a CNS cell line, CAD, in which morphological differentiation is initiated by serum deprivation. J Neurosci. 1997; 17:1217–1225. [PubMed: 9006967]

Ram PA, Waxman DJ. Role of the cytokine-inducible SH2 protein CIS in desensitization of STAT5b signaling by continuous growth hormone. J Biol Chem. 2000; 275:39487–39496. [PubMed: 10991939]

Ram PA, Waxman DJ. SOCS/CIS protein inhibition of growth hormone-stimulated STAT5 signaling by multiple mechanisms. J Biol Chem. 1999; 274:35553–35561. [PubMed: 10585430]

Rui L, Yuan M, Frantz D, Shoelson S, White MF. SOCS-1 and SOCS-3 block insulin signaling by ubiquitin-mediated degradation of IRS1 and IRS2. J Biol Chem. 2002; 277:42394–42398. [PubMed: 12228220]

Sancak Y, Peterson TR, Shaul YD, Lindquist RA, Thoreen CC, Bar-Peled L, Sabatini DM. The Rag GTPases bind raptor and mediate amino acid signaling to mTORC1. Science. 2008; 320:1496–1501. [PubMed: 18497260]

Starr R, Willson TA, Viney EM, Murray LJ, Rayner JR, Jenkins BJ, Gonda TJ, Alexander WS, Metcalf D, Nicola NA, Hilton DJ. A family of cytokine-inducible inhibitors of signalling. Nature. 1997; 387:917–921. [PubMed: 9202125]

Stewart SA, Dykxhoorn DM, Palliser D, Mizuno H, Yu EY, An DS, Sabatini DM, Chen IS, Hahn WC, Sharp PA, Weinberg RA, Novina CD. Lentivirus-delivered stable gene silencing by RNAi in primary cells. Rna. 2003; 9:493–501. [PubMed: 12649500]

Steyn FJ, Anderson GM, Grattan DR. Hormonal regulation of suppressors of cytokine signaling (SOCS) messenger ribonucleic acid in the arcuate nucleus during late pregnancy. Endocrinology. 2008; 149:3206–3214. [PubMed: 18325991]

Tauchi T, Yoshimura A, Ohyashiki K. CIS1, a cytokine-inducible SH2 protein, suppresses BCR/ABL-mediated transformation. Involvement of the ubiquitin proteasome pathway. Exp Hematol. 2001; 29:356–361. [PubMed: 11274764]

Tollet-Egnell P, Flores-Morales A, Stavreus-Evers A, Sahlin L, Norstedt G. Growth hormone regulation of SOCS-2, SOCS-3, and CIS messenger ribonucleic acid expression in the rat. Endocrinology. 1999; 140:3693–3704. [PubMed: 10433229]

Toniato E, Chen XP, Losman J, Flati V, Donahue L, Rothman P. TRIM8/GERP RING finger protein interacts with SOCS-1. J Biol Chem. 2002; 277:37315–37322. [PubMed: 12163497]

Tonko-Geymayer S, Goupille O, Tonko M, Soratroi C, Yoshimura A, Streuli C, Ziemiecki A, Kofler R, Doppler W. Regulation and function of the cytokine-inducible SH-2 domain proteins, CIS and SOCS3, in mammary epithelial cells. Mol Endocrinol. 2002; 16:1680–1695. [PubMed: 12089360]

Verdier F, Chretien S, Muller O, Varlet P, Yoshimura A, Gisselbrecht S, Lacombe C, Mayeux P. Proteasomes regulate erythropoietin receptor and signal transducer and activator of transcription 5 (STAT5) activation. Possible involvement of the ubiquitinated Cis protein. J Biol Chem. 1998; 273:28185–28190. [PubMed: 9774439]

Yang XO, Zhang H, Kim BS, Niu X, Peng J, Chen Y, Kerketta R, Lee YH, Chang SH, Corry DB, Wang D, Watowich SS, Dong C. The signaling suppressor CIS controls proallergic T cell development and allergic airway inflammation. Nat Immunol. 2013; 14:732–740. [PubMed: 23727894]

Yip SH, Eguchi R, Grattan DR, Bunn SJ. Prolactin signalling in the mouse hypothalamus is primarily mediated by signal transducer and activator of transcription factor 5b but not 5a. J Neuroendocrinol. 2012; 24:1484–1491. [PubMed: 22775396]

Yoshimura A, Ohkubo T, Kiguchi T, Jenkins NA, Gilbert DJ, Copeland NG, Hara T, Miyajima A. A novel cytokine-inducible gene CIS encodes an SH2-containing protein that binds to tyrosine-phosphorylated interleukin 3 and erythropoietin receptors. Embo J. 1995; 14:2816–2826. [PubMed: 7796808]

Zhang JG, Farley A, Nicholson SE, Willson TA, Zugaro LM, Simpson RJ, Moritz RL, Cary D, Richardson R, Hausmann G, Kile BJ, Kent SB, Alexander WS, Metcalf D, Hilton DJ, Nicola NA, Baca M. The conserved SOCS box motif in suppressors of cytokine signaling binds to elongins B and C and may couple bound proteins to proteasomal degradation. Proc Natl Acad Sci U S A. 1999; 96:2071–2076. [PubMed: 10051596]

Zhang W, Cheng GZ, Gong J, Hermanto U, Zong CS, Chan J, Cheng JQ, Wang LH. RACK1 and CIS mediate the degradation of BimEL in cancer cells. J Biol Chem. 2008; 283:16416–16426. [PubMed: 18420585]

Highlights

- Each CIS lysine residue can act as a substrate for ubiquitin attachment.
- Ubiquitination of CIS is not dependent on interactions with Elongin B/C proteins.
- Ubiquitination and Elongin B/C interactions both modulate CIS protein stability.
- Elongin B/C interactions contribute to CIS inhibition of prolactin receptor signaling.

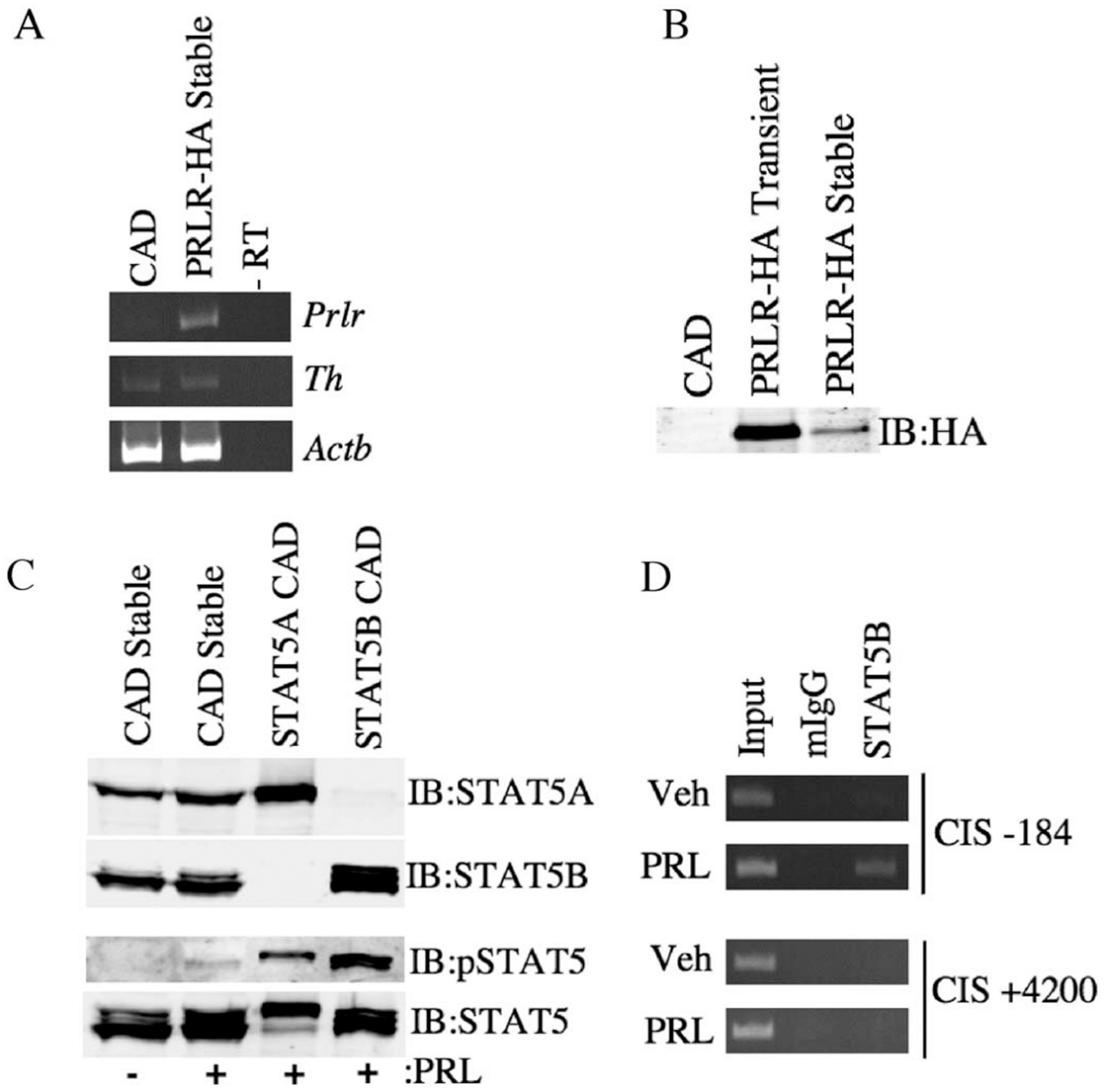

Fig. 1.

PRLR signaling pathways are active in PRLR-HA stable CAD cells. *A*, RNA (1 μg) isolated from PRLR-HA CAD stable cells was reverse transcribed and used in PCR reactions for rat *Prlr*, tyrosine hydroxylase (*Th*), and actin (*Actb*). *B*, Lysates from CAD (50 μg), CAD cells (10 μg) transiently transfected with PRLR-HA expression constructs and PRLR-HA CAD stable cells (50 μg) were analyzed by Western blot using anti-HA antibodies. *C*, Lysates from PRLR-HA CAD stable cells (60 μg) and CAD cells (3 μg) transiently transfected with PRLR and STAT5B or STAT5A expression constructs treated with vehicle or rPRL for 30 min were analyzed by Western blot using anti-STAT5B, anti- STAT5A, anti-pSTAT5 and

anti-STAT5 antibodies. *D*, ChIP analysis of STAT5B interaction with the CIS promoter. PRLR-HA stable CAD cells were treated with vehicle or rPRL for 1 hr followed by ChIP analysis using mIgG (control) and anti-STAT5B antibodies followed by PCR with −184 and +4200 *Cis* gene primer sets.

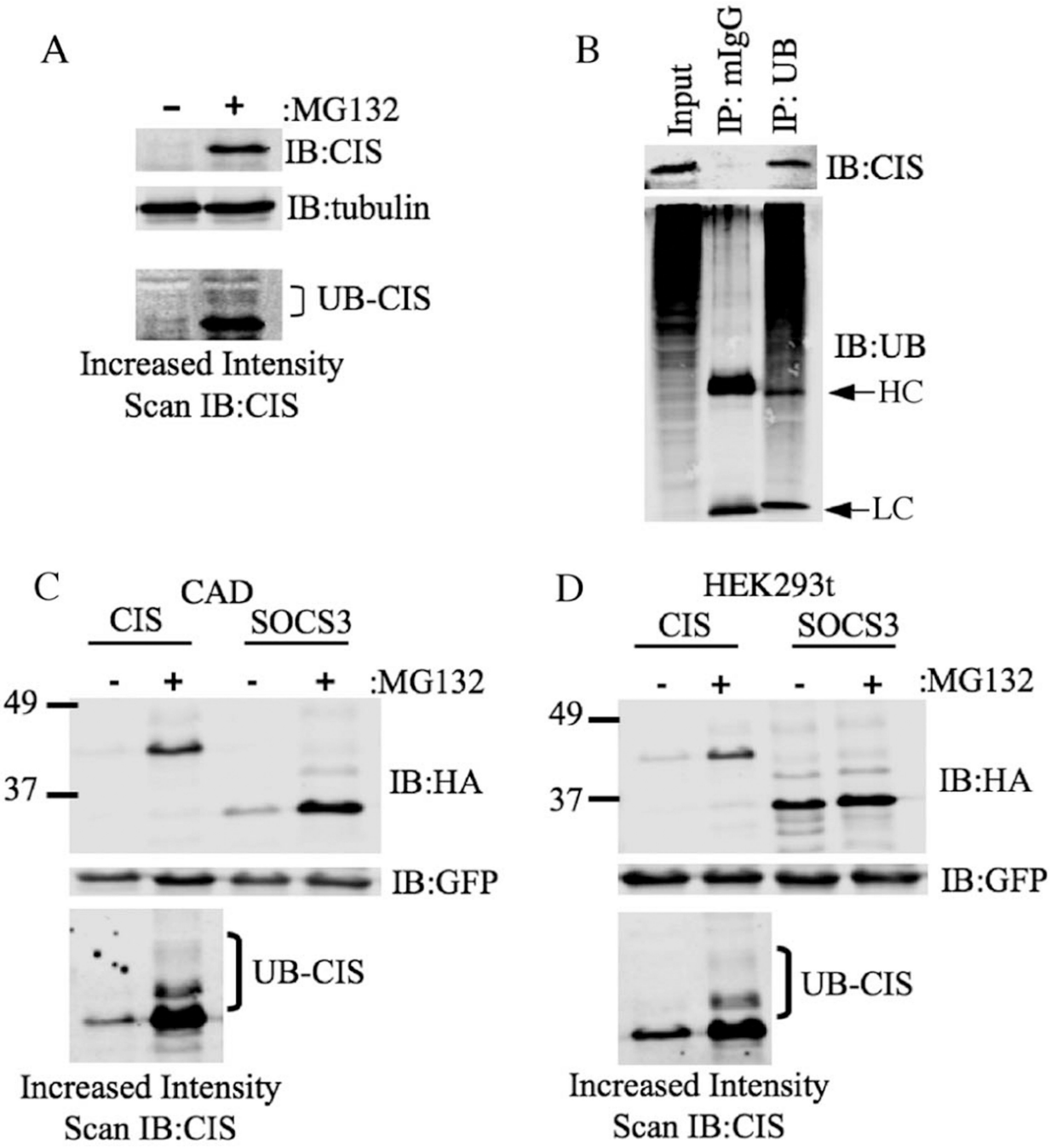

Fig. 2.

CIS is degraded and interacts with ubiquitin. *A*, PRLR-HA CAD stable cells were treated with PRL and DMSO (−) or MG132 (+) for 18 hrs. Lysates (50 μg) were analyzed by Western blot using anti-CIS and anti-tubulin antibodies. An increased intensity scan is also shown for the anti-CIS blot. *B*, Lysates from PRLR-HA CAD stable cells treated with PRL and MG132 were immunoprecipitated with normal mouse IgG or anti-ubiquitin antibodies followed by Western blot of input and immunoprecipitants with anti-ubiquitin and anti-CIS. Closed arrows on right indicate heavy chain (HC) and light chain (LC) IgG. *C*, CAD and *D*,

HEK 293t cells were transfected with GFP and HA-CIS, or HA-SOCS3 and then treated with vehicle or MG132 for 18 hrs. Lysates (30 μg) were analyzed by Western blot to determine HA-CIS, HA-SOCS3 and GFP levels using anti-HA and anti-GFP antibodies. Increased intensity scans are also shown for anti-HA blots. UB (ubiquitin).

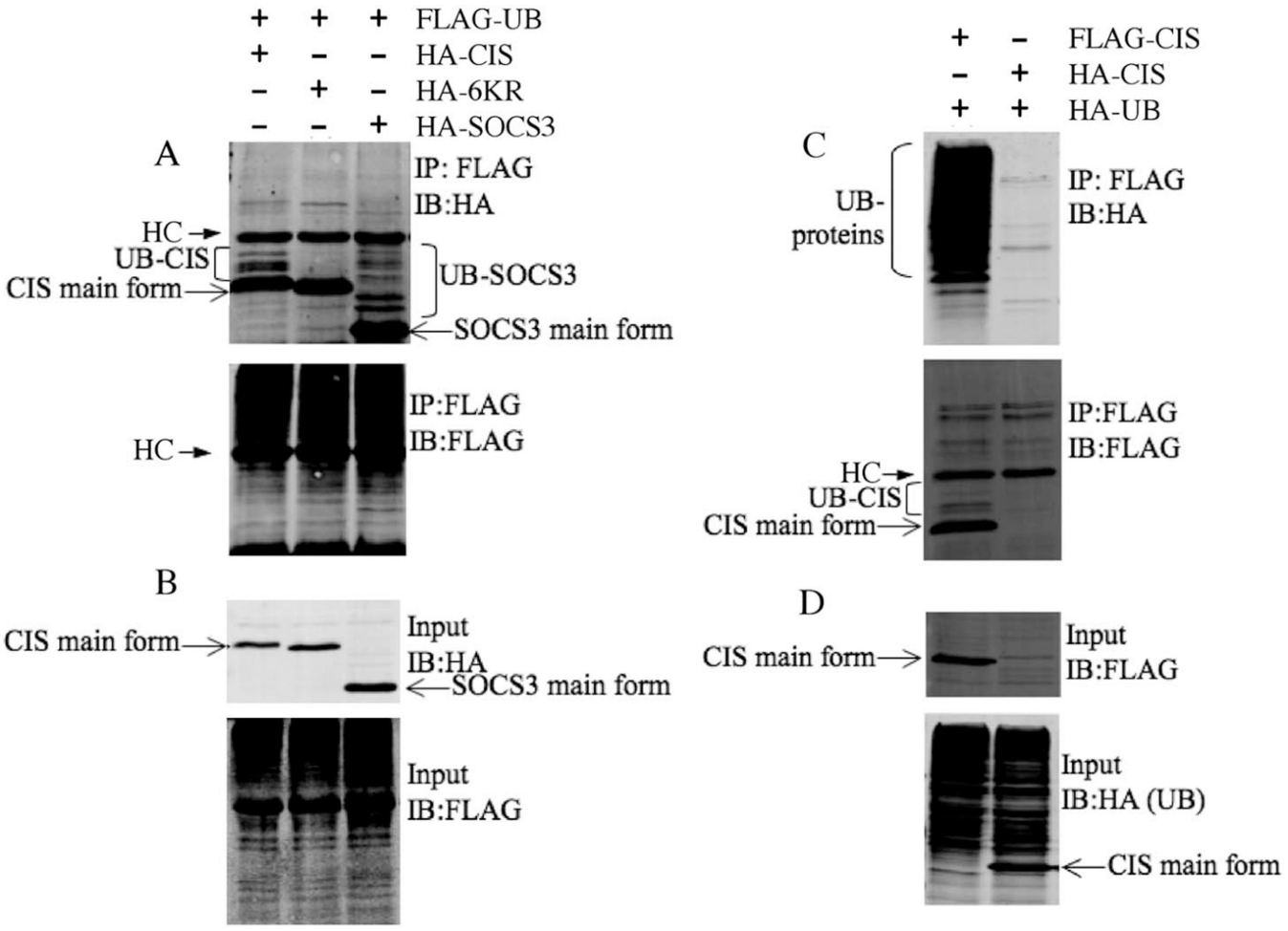

Fig. 3.

CIS is ubiquitinated. *A and B*, HEK 293t cells were transfected with combinations of the indicated FLAG-ubiquitin with HA-CIS, HA-6KR or HA-SOCS3 expression constructs, as indicated in the matrix above *A*, and treated with MG132. Cell lysates were immunoprecipitated with anti-FLAG beads followed by Western blot analysis of both immunoprecipitants (*A*) and inputs (*B*) with anti-HA (CIS and SOCS3) and anti-FLAG (ubiquitin). *C and D*, HEK 293t cells were transfected with combinations of the indicated FLAG-CIS or HA-CIS with HA-ubiquitin expression constructs, as indicated in the matrix above *C*, and treated with MG132. Cell lysates were immunoprecipitated with anti-FLAG beads followed by Western blot analysis of both immunoprecipitants (*C*) and inputs (*D*) with anti-HA (ubiquitin or CIS) and anti-FLAG (CIS). Closed arrows on the left indicate heavy chain IgG (HC). UB (ubiquitin).

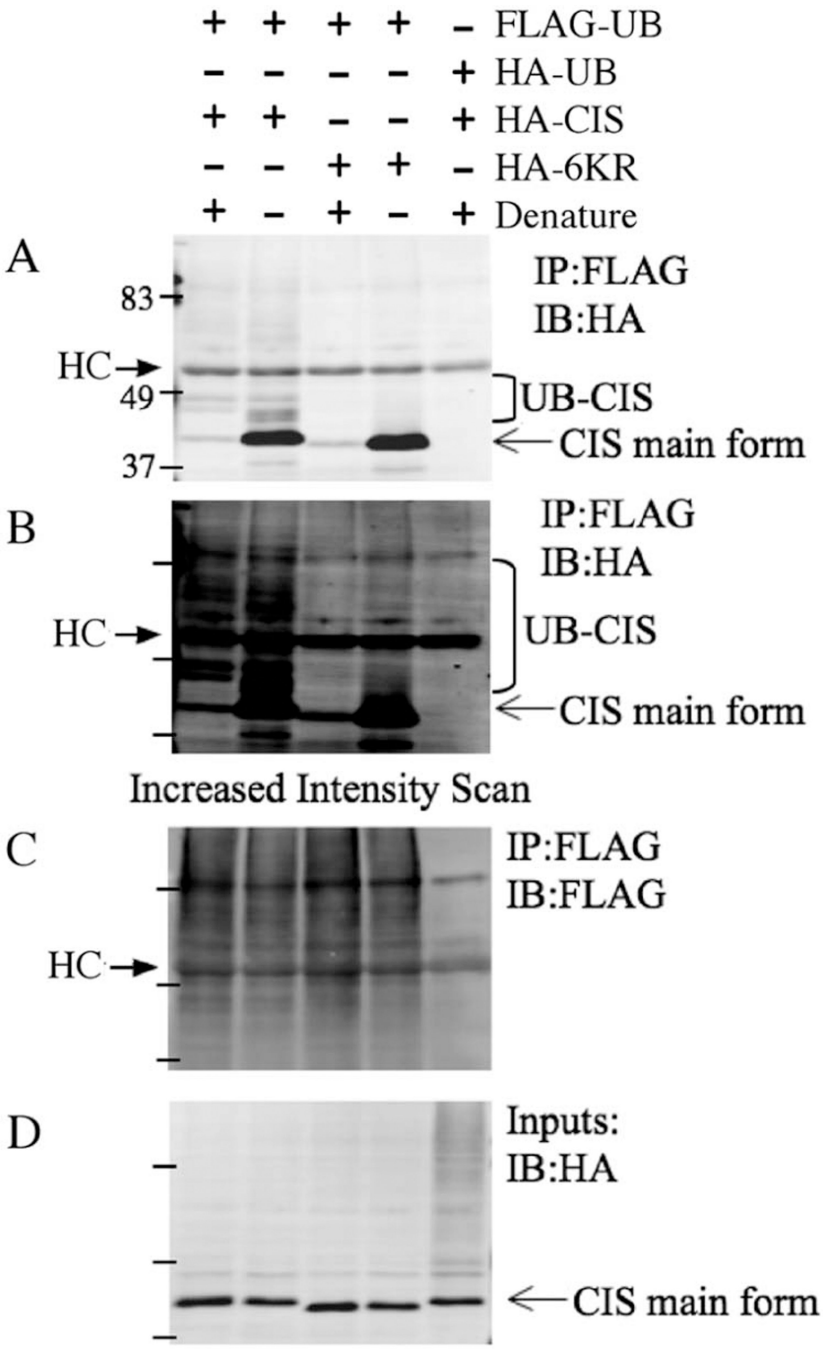

Fig. 4.

Covalent and non-covalent interactions of CIS with ubiquitin. *A–D*, HEK 293t cells were transfected with combinations of the indicated FLAG-ubiquitin or HA-ubiquitin with HA-CIS or HA-6KR expression constructs as shown in the matrix above *A* and treated with MG132. Lysates were prepared in either denaturing or naturing conditions followed by immunoprecipitations under identical conditions with anti-FLAG agarose beads. Western blots were performed on immunoprecipitants (*A*,*B*,*C*) and inputs (*D*) using anti-HA (*A*,*B*,*D*) or anti-FLAG (*C*). *B*, An increased intensity scan is also shown for the IP:FLAG; IB:HA

blot shown in panel *A*. Closed arrows on the left indicate heavy chain IgG (HC). UB (ubiquitin).

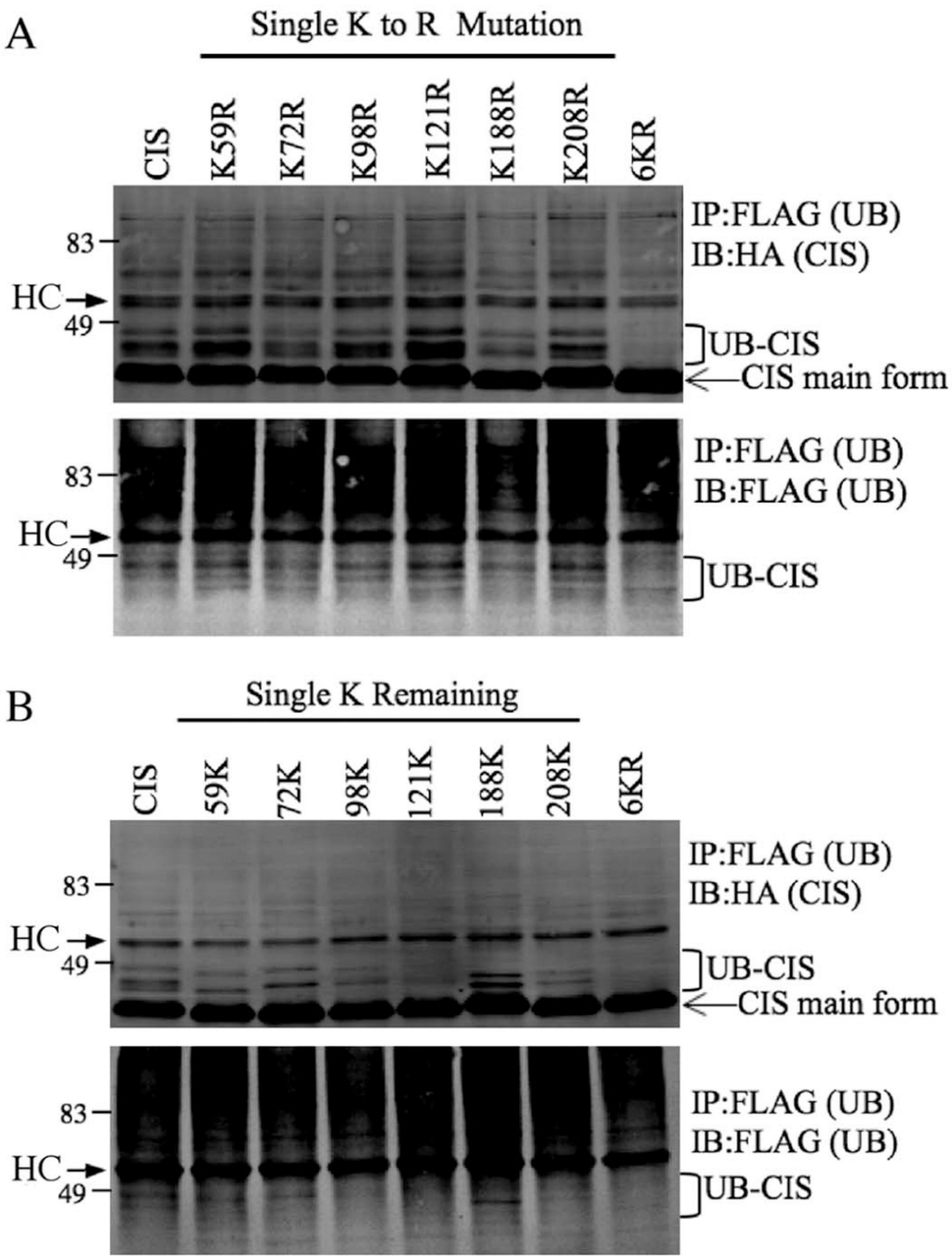

Fig. 5.

CIS is ubiquitinated on each lysine residue. HEK 293t cells were transfected with FLAG-ubiquitin with HA-CIS, (*A*) HA-CIS with single lysine to arginine mutations, (*B*) HA-CIS mutants containing only one lysine at the indicated position with the other five lysine mutated to arginines or HA-6KR expression constructs and treated with MG132. Cell lysates were immunoprecipitated with anti-FLAG agarose beads followed by Western blot analysis of immunoprecipitants with anti-HA and anti-FLAG. Open arrows on the right indicate main

form of CIS. Brackets on the right indicate higher molecular weight CIS proteins. Closed arrows on the left indicate heavy chain IgG (HC). UB (ubiquitin).

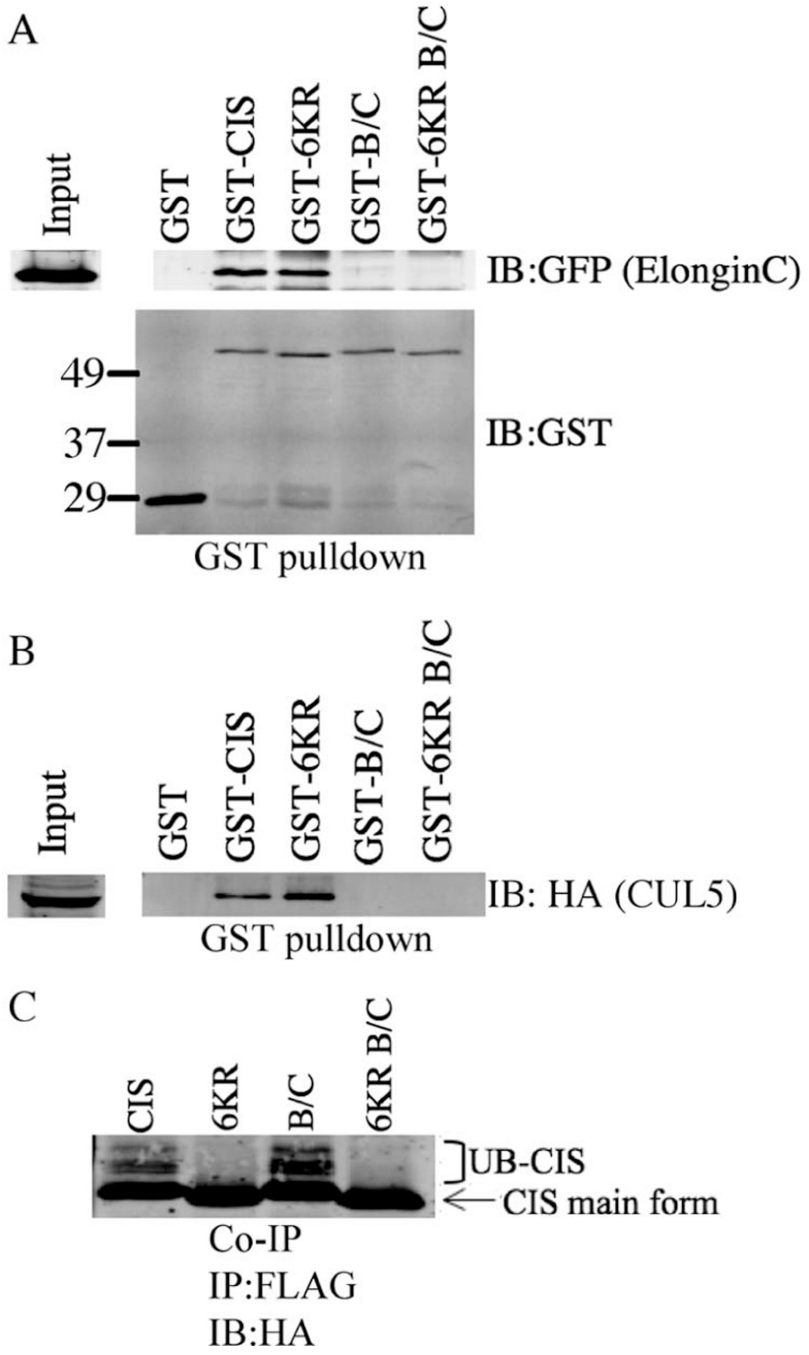

Fig. 6.

CIS B/C box is not necessary for CIS ubiquitination. *A and B*, Lysates from (*A*) YFP-Elongin C or (*B*) HA-CUL5 transfected HEK 293t cells were incubated with recombinant GST or the indicated GST-CIS proteins bound to glutathione beads. Eluted proteins were analyzed by Western blot using anti-GFP (YFP-Elongin C) or anti-HA (CUL5) and anti-GST (GST or GST-CIS). *C*, HEK 293t cells were transfected with FLAG-ubiquitin and HA-CIS, 6KR, B/C (mutated Elongin B/C box), or 6KR B/C (all lysines mutated to arginines with Elongin B/C box mutation). Cell lysates were immunoprecipitated with anti-FLAG

agarose beads followed by Western blot analysis with anti-HA. Bracket indicates higher molecular weight CIS proteins. UB (ubiquitin).

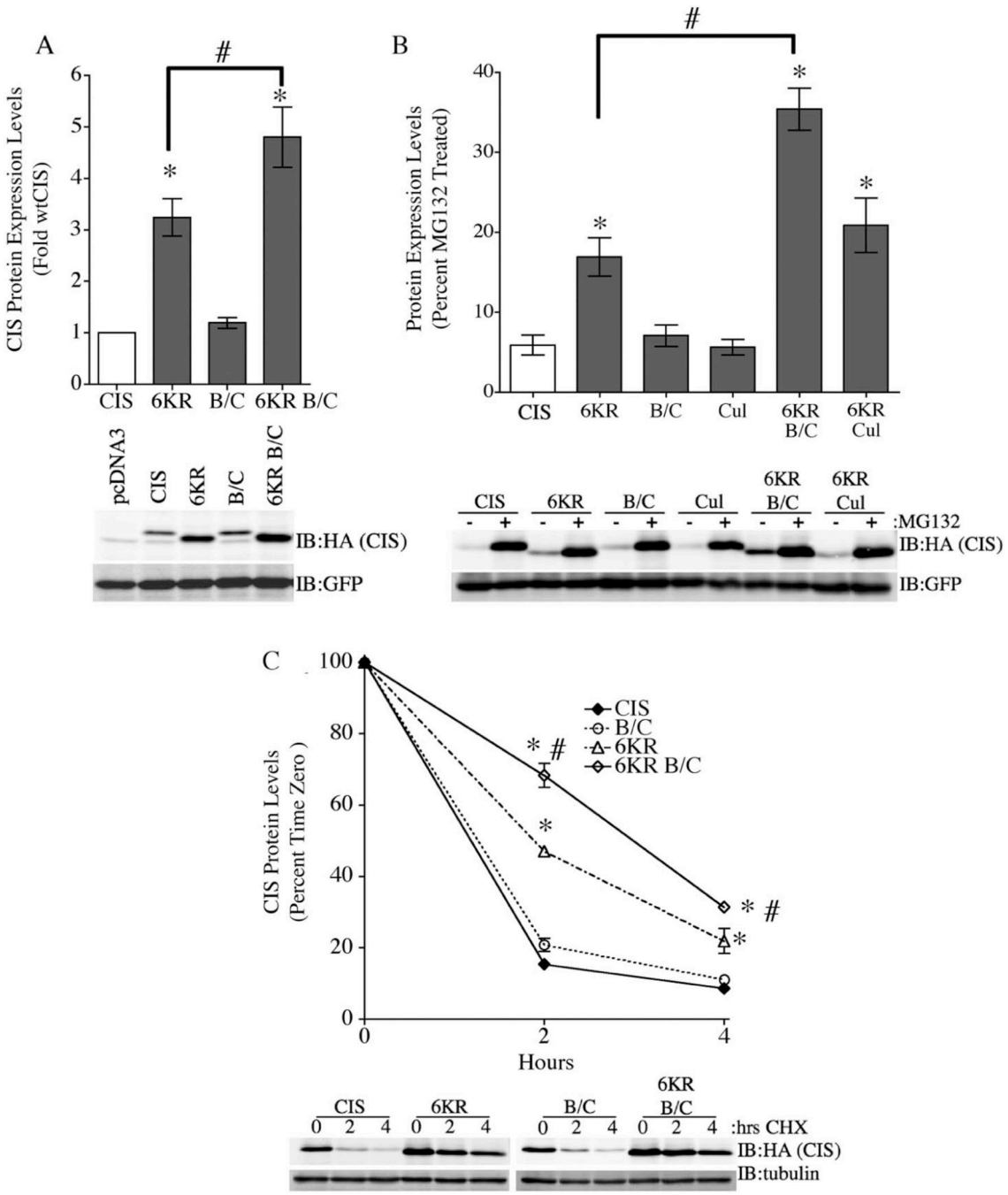

Fig. 7.

Influence of CIS ubiquitination and Elongin B/C interaction on CIS protein stability. *A*, HEK 293t cells were co-transfected with GFP and pcDNA3, HA-CIS, HA-6KR, HA-B/C or HA-6KR B/C expression constructs. Lysates were collected 24 hrs later and analyzed by Western blot using anti-HA and anti-GFP antibodies. CIS levels were normalized to GFP and fold changes in expression levels due to the mutations were determined by comparison to HA-CIS, which was set to 1. *B*, HEK 293t cells were co-transfected with GFP and the indicated HA-CIS construct. Cells were treated with vehicle or MG132 for 18 hrs and

lysates were analyzed by Western blot using anti-HA and anti-GFP antibodies. CIS levels were normalized to GFP and the percentage of vehicle CIS to MG132 CIS was determined for each CIS construct. *C*, HEK 293t cells were transfected with the indicated HA-CIS construct and treated with cycloheximide (CHX) for the indicated times. Lysates were analyzed by Western blot using anti-HA and anti-β-tubulin. CIS levels were first normalized to β-tubulin levels and 2 and 4 hr levels were compared to 0 hr (set to 100% for each mutant) to determine the percentage of CIS levels at each time point. Values represent the mean ± SE of three to seven independent experiments. *P < 0.05 versus CIS. #P < 0.05 6KR versus 6KR B/C. Representative blots are also shown.

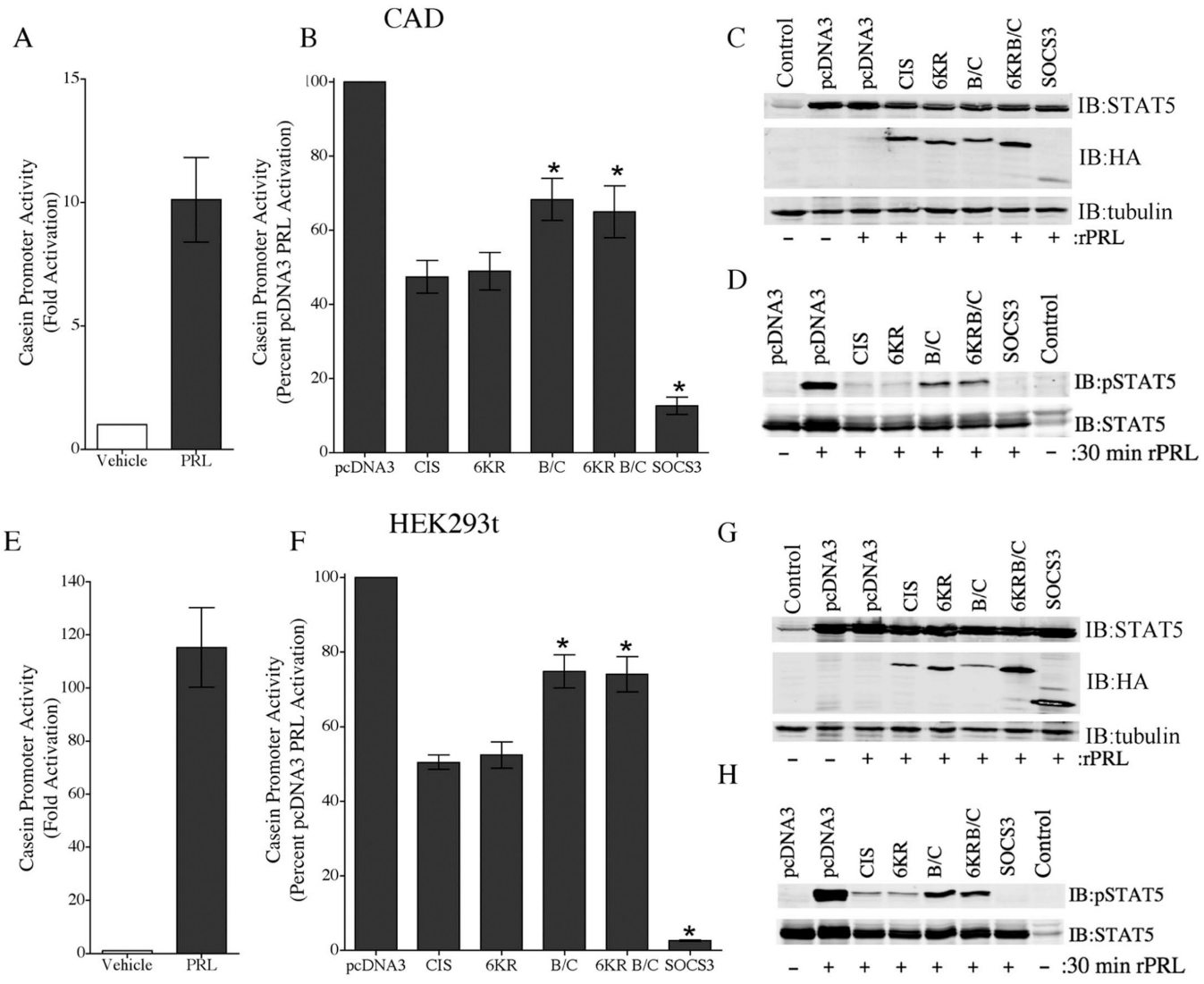

Fig. 8.

CIS inhibition of PRLR-STAT5b signaling is dependent on Elongin B/C interactions and not CIS ubiquitination. CAD (*A, B, C*) and HEK 293t (*E, F, G*) cells were transfected with PRLR, STAT5B and casein (−344 to −1 bp) promoter-luciferase reporter together with pcDNA3, CIS, 6KR, B/C, 6KR B/C, or SOCS3 expression constructs. The pcDNA3-transfected cells were treated with vehicle or rPRL and CIS- and SOCS3-transfected cells were treated with rPRL followed by dual luciferase assays. *A and E*, Fold activations were first determined by comparing rPRL to vehicle-treated values for the pcDNA3-transfected cells. *B and F*, The pcDNA3 fold activation was then set to 100% and the percentage of casein promoter activation was determined for CIS and SOCS3 transfected cells for each independent experiment. Values represent the mean ± SE of four or seven independent experiments. *P < 0.05 versus CIS. *C and G*, Western blot analysis on 15 μL of lysates used for luciferase assays to demonstrate expression levels of STAT5, CIS and SOCS3 relative to tubulin. *D and H*, Western blot analysis on lysates from CAD (*D*) and HEK293t (*H*) cells transfected with PRLR and STAT5B with pcDNA3, CIS, 6KR, B/C, 6KR B/C, or SOCS3

expression constructs to determine the influence of CIS or the various CIS mutant on 30 min PRL-stimulated pSTAT5 levels. Control lanes are lysates from untransfected cells.

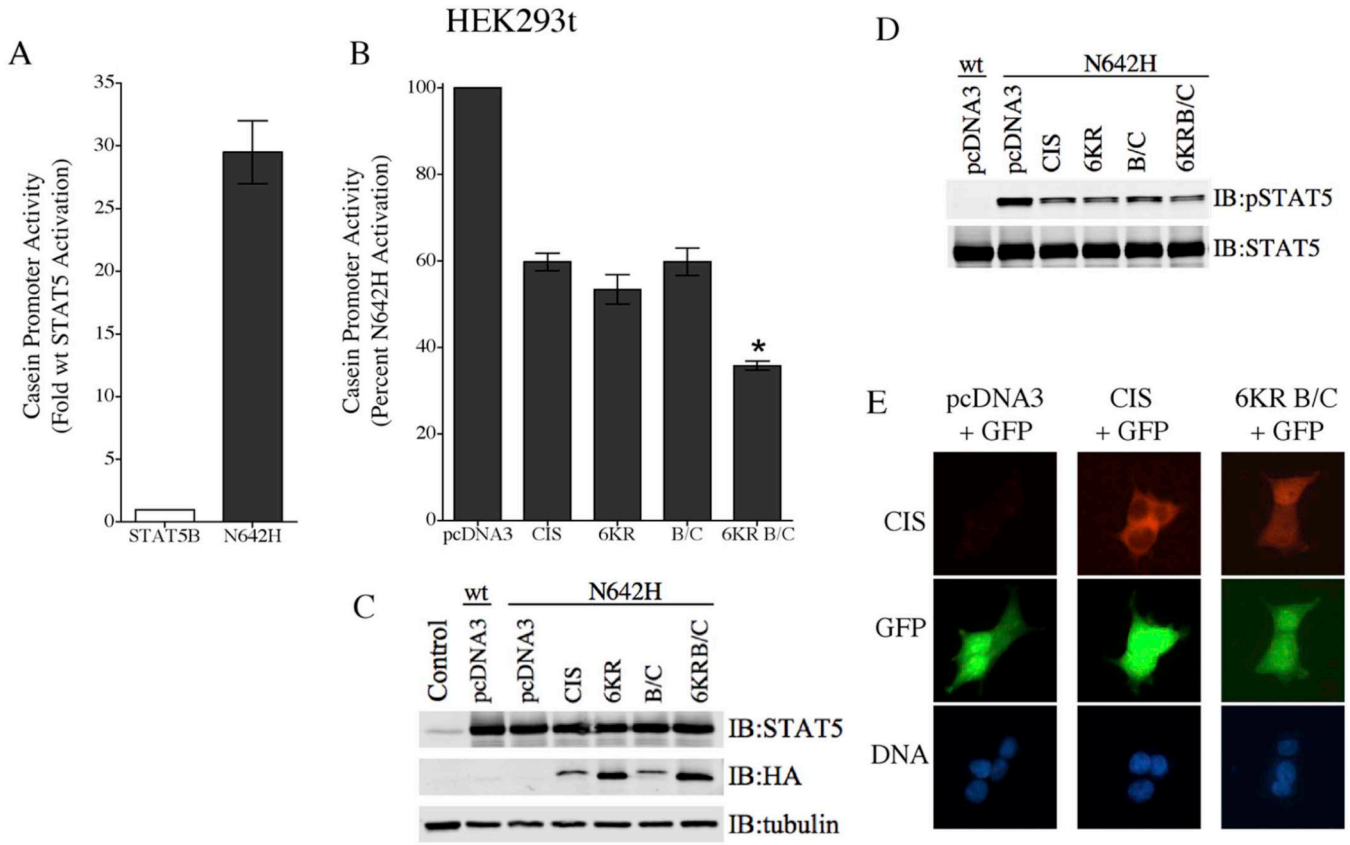

Fig. 9.

CIS inhibition of constitutively active STAT5B. *A and B*, HEK 293t cells were transfected with casein promoter-luciferase construct and STAT5B or STAT5B (N642H) together with pcDNA3, CIS, 6KR, B/C, or 6KR B/C expression constructs followed by dual luciferase assays. *A*, Fold activations were first determined by comparing STAT5B to N642H values in the pcDNA3 co-transfected cells. *B*, The N642H pcDNA3 co-transfected fold activation was then set to 100% and the percentage of activation was determined for the indicated CIS co-transfected cells for each independent experiment. Values represent the mean ± SE of four independent experiments. *P < 0.05 versus CIS. *C*, Western blot analysis on 15 μL of lysates used for luciferase assays to demonstrate expression levels of STAT5, CIS and SOCS3 relative to tubulin. *D*, Western blot analysis on lysates from cells transfected with STAT5B (wt) or STAT5B (N642H) together with pcDNA3, CIS, 6KR, B/C, or 6KR B/C expression constructs determine the influence of CIS or the various CIS mutant on pSTAT5 levels. *E*, HEK 293t cells were transfected with GFP and pcDNA3, CIS or 6KR B/C constructs. CIS localization was determined by immunofluorescence using anti-CIS.